ESAIM: M2AN 51 (2017) 2127–2158
DOI: 10.1051/m2an/2017014

ESAIM: Mathematical Modelling and Numerical Analysis
www.esaim-m2an.org

SOME *A POSTERIORI* ERROR BOUNDS FOR REDUCED-ORDER MODELLING OF (NON-)PARAMETRIZED LINEAR SYSTEMS

Lihong Feng[1], Athanasios C. Antoulas[2] and Peter Benner[1]

Abstract. We propose *a posteriori* error bounds for reduced-order models of non-parametrized linear time invariant (LTI) systems and parametrized LTI systems. The error bounds estimate the errors of the transfer functions of the reduced-order models, and are independent of the model reduction methods used. It is shown that for some special non-parametrized LTI systems, particularly efficiently computable error bounds can be derived. According to the error bounds, reduced-order models of both non-parametrized and parametrized systems, computed by Krylov subspace based model reduction methods, can be obtained automatically and reliably. Simulations for several examples from engineering applications have demonstrated the robustness of the error bounds.

Mathematics Subject Classification. 37M05, 65P99, 65L70, 65L80.

Received January 20, 2016. Revised March 15, 2017. Accepted March 16, 2017.

1. Introduction

The technique of model order reduction (MOR) has been successfully applied in many fields, *e.g.*, mechanical engineering, structural engineering, fluid dynamics, optimization, control, circuit simulation, microelectromechanical systems (MEMS) simulation, uncertainty quantification, inverse problems etc.. The robustness of MOR has been revealed in all the above application areas.

The purpose of MOR is to reduce the number of degrees of freedom in the original large-scale systems described by algebraic equations, ordinary differential equations (ODEs), or differential algebraic equations (DAEs) while attaining good accuracy. These systems usually come from (time-)spatial discretization of partial differential equations describing the underlying process, devices, structure or dynamics, etc.. Sometimes, the mathematical models are described directly by ODEs/DAEs, for example, the many models obtained based on modified nodal analysis (MNA) in circuit or MEMS simulation.

Parametric model order reduction (PMOR) is an advanced MOR technique for more complex mathematical models, where some variables, called parameters, are entries of the system matrices that are allowed to vary, such that the systems are parametrized. For a parametrized system, PMOR methods aim to preserve the parameters as symbolic quantities in the reduced-order models, such that a single reduced-order model is sufficiently accurate for all possible variations of the parameters.

Keywords and phrases. Model order reduction, error estimation.

[1] Max Planck Institute for Dynamics of Complex Technical Systems, Sandtorstrasse 1, 39106 Magdeburg, Germany. feng@mpi-magdeburg.mpg.de; benner@mpi-magdeburg.mpg.de

[2] Department of Electrical and Computer Engineering, Rice University, Houston. aca@rice.edu

Krylov subspace based moment-matching MOR and Gramian based MOR are popular MOR methods for non-parametrized LTI systems. The very basic method of Gramian based MOR is balanced truncation, which is well-known for its global error bound. Recent algorithmic progress has made this method applicable to truly large-scale systems, see, *e.g.*, [7]. As these advances include certain approximations, the global error bound is not computable exactly, and therefore should be confirmed by an *a posteriori* error bound. Moment-matching MOR methods are computationally efficient, and are widely used in large-scale problems arising from circuit or MEMS simulation. However, they suffer from the lack of a global error bound, which leads to the fact that the reduced-order model cannot be generated automatically and reliably.

Some attempts have been made to get error estimation for moment-matching MOR methods applied to non-parametrized LTI systems [8,12,20,29,33,43]. While showing the efficiency of their error estimators, these are more or less heuristics [8,12,20,29,33]. Based on systems theory, an error bound is derived in [43], but faces high computational complexity. The residual of the state vector is simply used in [29] as the error estimator of the reduced-order model. All these error estimators are limited to non-parametrized systems. An *a posteriori* error bound for parametrized LTI systems is proposed in time domain in [30]. Although it is stated that it can be seen as *a posteriori* error bound for the Krylov subspace based method (*e.g.* moment-matching MOR), it is hardly computable

In recent years, numerous model order reduction methods for parametrized LTI systems have been developed, for example, the Krylov subspace based (multi-moment matching) PMOR methods [16,18,19,21], the interpolation based PMOR methods [3,5,6,37], the Loewner approach to parametric model reduction [35], and the reduced basis methods [14,28]. A survey of PMOR methods can be found in [10]. Among these methods, only for the reduced basis method *a posteriori* error bounds are known. These enable automatic generation of a reliable reduced parametrized model.

Error bounds/estimators have been intensively studied in the context of the reduced basis method for parametrized systems. Many error estimators developed for the reduced basis methods estimate the error in the state vectors (field variables) [24,31,32,40], not for the outputs of the systems. In many applications, the output or the transfer function (output in the frequency domain) of the system are of interest. The error estimations for the state vectors often tends to overestimate the output errors. Nevertheless, output error estimators for reduced basis methods are proposed in [39,42], which are only applicable to steady state systems. In [25], an output error bound for linear parabolic equations is proposed, which estimates the output error of the reduced-order model in time domain. Output error bounds in time domain are also introduced in [48–50] based on space-time variational formulation of the original system. Output error estimation in time domain for projection based MOR and for general nonlinear systems is proposed in [51]. However, direct application of those time-domain error bounds to the frequency-domain PMOR methods, such as the Krylov subspace based multi-moment matching PMOR methods [16,18,19,21], is unclear. Typically, almost all the error bounds for the reduced basis methods necessitate the bilinear forms of the PDE models [24,25,28,31,32,39,42,48–50].

The above observations motivate us to derive output error bounds for dynamical systems in the discretized vector space $\mathbb{C}^n$. We propose several *a posteriori* error bounds for the reduced-order models of both, non-parametrized LTI systems and parametrized LTI systems. The error bounds are the bounds for the difference between the transfer function of the original system and that of the reduced-order model, and are applicable to (P)MOR methods based on Petrov−Galerkin projection [16,18,19,21] and other methods that allow efficient residual evaluation of the output quantities.

The basic idea of the proposed error bounds originates from the output error bounds for the reduced basis methods [14,39,42]. The main theoretical contributions of the newly derived error bounds are firstly, the error bounds are independent of the discretization method (finite difference, finite element, finite volume) applied to the original PDEs. Secondly, the error bounds can be directly used in the discretized vector space $\mathbb{C}^n$, without going back to the PDEs, and especially to the bilinear form (weak formulation) associated with the finite element discretization. This is typically useful when only discretized systems are available in some situations. In particular, most of the dynamical models in circuit and MEMS simulation are derived using commercial

software, where the usable mathematical models appear directly as ordinary differential equations (ODEs), or differential algebraic equations (DAEs). The bilinear form of the PDE models are usually unknown.

Technically, the proposed error bounds provide a way of automatically generating reliable reduced-order models computed by the Krylov subspace based (P)MOR methods, which is desired in design automation for circuits and MEMS. Although Krylov subspace based (P)MOR methods have been integrated into some simulation tools [41], the reduced-order model cannot be guaranteed to satisfy the required accuracy due to the lack of an robust error bound. We are making the design automation reliable by proposing some *a posteriori* error bounds for both non-parametrized and parametrized linear systems.

The paper is organized as follows. In the next section, we present the transfer function of an LTI system, and the reduced transfer function of the reduced-order model. Our goal is to propose error bounds for the error between the two transfer functions. We further show several examples of LTI systems, for which the error of the corresponding reduced-order models can be measured by the proposed error bounds. In Section 3, we propose an *a posteriori* error bound which has strong limitations on the system matrices. *a posteriori* error bounds for more general LTI systems are proposed in Section 4. How to efficiently compute the error bounds is discussed in Section 5. Section 6 relates the error bound analysis in Section 4 to a new reduction method. In the section that follows, the basic idea of moment-matching MOR/multi-moment matching PMOR methods are reviewed. One will see that automatic generation of reduced-order models relies on adaptive selection of expansion points. Algorithms for automatic selection of the expansion points according to the *a posteriori* error bounds are proposed. Simulation results are presented in Section 8. Conclusions and future work are given in the end.

2. Preliminaries

In this paper, we consider *a posteriori* error bounds for model order reduction of LTI systems, whose transfer functions are of the form

$$H(\mu) = C(\mu)G^{-1}(\mu)B(\mu). \tag{2.1}$$

where $\mu := (\mu_1, \ldots, \mu_p)^T \in \mathbb{C}^p$ is a vector of parameters or a vector of functions of parameters, *e.g.*, $\mu_i := \phi_i(p_1, \ldots, p_q) : \mathbb{C}^q \mapsto \mathbb{C}, i = 1, \ldots, p$. $B(\mu) \in \mathbb{R}^{n\times m_1}$ is the input matrix associated with the input signal $u(t) \in \mathbb{R}^{m_1}$, $C(\mu) \in \mathbb{R}^{m_2\times n}$ is the output matrix defining the output response $y(t, \mu)$, and $G(\mu)$ has different forms depending on the systems considered, see the examples below. Assume that the transfer function of the reduced-order model is,

$$\hat{H}(\mu) = \hat{C}(\mu)\hat{G}^{-1}(\mu)\hat{B}(\mu), \tag{2.2}$$

the goal of this paper is to present some *a posteriori* error bounds $\Delta(\mu)$, so that

$$\|H(\mu) - \hat{H}(\mu)\|_{\max} \le \Delta(\mu), \tag{2.3}$$

where $\|\cdot\|_{\max}$ denotes the max norm of a matrix, $\hat{B}(\mu) \in \mathbb{R}^{r\times m_1}, \hat{C}(\mu) \in \mathbb{R}^{m_2\times r}$, $\hat{G}(\mu) \in \mathbb{R}^{r\times r}$. We consider general multiple-input and multiple-output (MIMO) systems, *i.e.* $m_1 \ge 1$ and $m_2 \ge 1$.

2.1. Systems that can be evaluated *via* the proposed error bounds

We consider several examples of the systems whose reduced-order models can be evaluated *via* the proposed error bounds for the transfer function. Firstly, the transfer function of a first-order LTI system, *e.g.*,

$$\begin{aligned} E(\tilde{\mu})\frac{\mathrm{d}x(t,\tilde{\mu})}{\mathrm{d}t} &= A(\tilde{\mu})x(t,\tilde{\mu}) + B(\tilde{\mu})u(t),\\ y(t,\tilde{\mu}) &= C(\tilde{\mu})x(t,\tilde{\mu}), \end{aligned} \tag{2.4}$$

can be written as in (2.1), with $G(\mu) = sE(\tilde{\mu}) - A(\tilde{\mu})$. Here and below, the entries in μ could be certain functions of the geometrical or physical parameters $\tilde{\mu} := (\tilde{\mu}_1, \ldots, \tilde{\mu}_{\tilde{p}})^T \in \mathcal{D} \subset \mathbb{R}^{\tilde{p}}$ and the Laplace variable s,

e.g., $\mu_i := \phi_i(\tilde{\mu}_1, \ldots, \tilde{\mu}_{\tilde{p}}, s)$, where $\mathcal{D}$ is the feasible parameter domain. $E(\tilde{\mu}) \in \mathbb{R}^{n\times n}, A(\tilde{\mu}) \in \mathbb{R}^{n\times n}$ are the system matrices. $x \in \mathbb{R}^n$ is the state vector.

Secondly, second-order LTI systems,

$$\begin{aligned} M(\tilde{\mu})\frac{d^2x(t,\tilde{\mu})}{\mathrm{d}t^2} + K(\tilde{\mu})\frac{\mathrm{d}x(t,\tilde{\mu})}{\mathrm{d}t} + A(\tilde{\mu})x(t,\tilde{\mu}) &= B(\tilde{\mu})u(t), \\ y(t,\tilde{\mu}) &= C(\tilde{\mu})x(t,\tilde{\mu}), \end{aligned} \tag{2.5}$$

have transfer functions $H(\mu)$ as in (2.1), with $G(\mu) = s^2M(\tilde{\mu}) + sK(\tilde{\mu}) + A(\tilde{\mu})$. Therefore, the error of the reduced-order model of either a first-order LTI system or a second-order LTI system can be evaluated via (2.3).

Finally, steady-state systems without time evolution can be written in the form

$$\begin{aligned} G(\tilde{\mu})x(\tilde{\mu}) &= B(\tilde{\mu}), \\ y(\tilde{\mu}) &= C(\tilde{\mu})x, \end{aligned} \tag{2.6}$$

The output $y(\tilde{\mu})$ of (2.6) has the same form as $H(\mu)$ in (2.1). Therefore, the output error of the reduced-order model of (2.6) can also be evaluated via (2.3), by replacing $H(\mu)$ with $y(\tilde{\mu})$, and $\hat{H}(\mu)$ with $\hat{y}(\tilde{\mu})$, the approximate output computed from its reduced-order model.

3. Error bound for special LTI systems

The technique of deriving the error bound in this section is motivated by the method in [39], where an output error bound for the reduced-order model is derived based on the weak formulation of certain PDEs. The error bound in [39] is derived in functional space, and is only valid for parametrized systems with real parameters. Here, we consider estimating the error of the reduced-order model directly in the vector space $\mathbb{C}^n$. Further extensions have been made, so that the derived error bound is applicable to systems with complex parameters, and finally, it can be used for adaptive selection of the multiple expansion points discussed in Section 7.1.1.

In Section 5, we will see that the error bound derived in this section is only valid for some special systems. For example, for non-parametrized systems with $G(\mu) = sE - A$, E is required to be symmetric positive definite, and A needs to be symmetric negative definite. For parametrized systems, there are more limitations on $G(\mu)$. This will be discussed in detail in Section 5.

3.1. Derivation of an error bound for SISO systems

We only consider single-input single-output (SISO) systems in this subsection. The results will be used to get an *a posteriori* error bound for MIMO systems in the next subsection.

To derive the error bound, we define the norm $\|\cdot\|_{\tilde{A}}$: $\mathbb{C}^n \to \mathbb{R}$ for a complex vector x as

$$\|x\|_{\tilde{A}} = (x^*\tilde{A}x)^{1/2}$$

Here, the matrix $\tilde{A}$ is assumed to be symmetric positive definite. In the following, no further assumptions on $\tilde{A}$ are made during the proofs of the propositions and theorems. It can be simply taken as the identity matrix, then the norm reduces to the standard 2-norm. x^* is the conjugate transpose of $x \in \mathbb{C}^n$. The norm $\|\cdot\|_{\tilde{A}}$ is actually associated with the inner product: $\langle\cdot,\cdot\rangle$: $\langle x_1, x_2\rangle = x_2^*\tilde{A}x_1,\ \forall x_1, x_2 \in \mathbb{C}^n$.

We also assume that the matrix-valued function $G(\mu)$: $\mathbb{C}^p \mapsto \mathbb{C}^{n\times n}$ satisfies the following coercivity conditions[3]

$$\mathrm{Re}(x^*G(\mu)x) \geq \alpha(\mu)(x^*\tilde{A}x), \forall x \in \mathbb{C}^n, x \neq 0, \mathrm{Re}(s) \geq 0, \forall \tilde{\mu} \in \mathcal{D} \subset \mathbb{R}^{\tilde{p}}. \tag{3.1}$$

[3]we assume that the systems considered are stable, *i.e.* the system eigenvalues λ for the system in (2.4), $[\lambda E(\tilde{\mu}) - A(\tilde{\mu})]x = 0$, and for the system in (2.5), $[\lambda^2 M(\tilde{\mu}) + \lambda K(\tilde{\mu}) + A(\tilde{\mu})]x = 0$, where $\tilde{\mu}$ is defined in (2.4), (2.5), are in the open left plane, $\forall\tilde{\mu}$. Note that the entries of the vector μ are functions of the parameters $\tilde{\mu}$ and the Laplace variable s, *i.e.* $\mu_i := \phi_i(\tilde{\mu}_1, \ldots, \tilde{\mu}_{\tilde{p}}, s)$, as defined in (4). As a result, to avoid defining $G(\mu)$ on the eigenvalues, we restrict s to be on the closed right half plane, *i.e.* $G(\mu)$ is assumed to satisfy (3.1) and (3.2), $\forall s$ on the closed right half plane: $\mathrm{Re}(s) \geq 0, \forall\tilde{\mu} \in \mathcal{D} \subset \mathbb{R}^{\tilde{p}}$. The domain $\mathcal{D}$ of the parameters $\tilde{\mu}$ may be any subset of $\mathbb{R}^{\tilde{p}}$, it is only implicitly restricted by the coercivity assumptions. That is, our results are valid only for those parameter domains $\mathcal{D}$ for which (3.1) and (3.2) are satisfied.

and

$$\mathrm{Im}(x^*G(\mu)x) \geq \gamma(\mu)(x^*\tilde{A}x), \forall x \in \mathbb{C}^n, x \neq 0, \mathrm{Re}(s) \geq 0, \forall \tilde{\mu} \in \mathcal{D} \subset \mathbb{R}^{\tilde{p}}. \tag{3.2}$$

where $\mathrm{Re}(\cdot)$ means the real part of $x^*G(\mu)x$, and $\mathrm{Im}(\cdot)$ it's imaginary part. $\alpha(\mu) > 0, \gamma(\mu) > 0$ may depend on the parameter μ. Efficient computation of $\alpha(\mu) > 0, \gamma(\mu) > 0$ is given in Section 5. Our goal is to derive an error bound for the error $|H(\mu) - \hat{H}(\mu)|$, where $|\cdot|$ means the absolute value or modulus of a complex number.

We first define an auxiliary primal system in the frequency domain,

$$\begin{aligned} G(\mu)x(\mu) &= B(\mu), \\ y(\mu) &= C(\mu)x(\mu), \end{aligned} \tag{3.3}$$

It is easy to see that the output $y(\mu)$ in (3.3) equals the transfer function $H(\mu)$ of the original system (2.1). Note that (3.3) is an instance of the original system for a particular input function (impulsive excitation). It is only used to derive the transfer function error bounds, and it is not the target of our consideration. Assume that the transfer function $\hat{H}(\mu)$ in (2.2) corresponds to the reduced matrices[4] $\hat{G}(\mu) = W^TG(\mu)V$, $\hat{B}(\mu) = W^TB(\mu)$, and $\hat{C}(\mu) = C(\mu)V$. Then the reduced-order model for the primal system (3.3) is defined as

$$\begin{aligned} W^TG(\mu)Vz(\mu) &= W^TB(\mu), \\ \hat{y}(\mu) &= C(\mu)Vz(\mu), \end{aligned} \tag{3.4}$$

where $W, V \in \mathbb{R}^{n\times r}$ are the matrices used to obtain $\hat{H}(\mu)$. Here $\hat{x}(\mu) := Vz(\mu)$ is the approximation of $x(\mu)$ in (3.3). Analogously, $\hat{y}(\mu)$ equals the transfer function $\hat{H}(\mu)$.

To assist the derivation of the error bound, we need a dual system in the frequency domain,

$$\begin{aligned} G^*(\mu)x^{du}(\mu) &= -C^*(\mu), \\ y^{du}(\mu) &= B^*(\mu)x^{du}(\mu). \end{aligned} \tag{3.5}$$

The reduced-order model for the dual system is defined as

$$\begin{aligned} V^TG^*(\mu)Wz^{du}(\mu) &= -V^TC^*(\mu), \\ \hat{y}^{du}(\mu) &= B^*(\mu)Wz^{du}(\mu), \end{aligned} \tag{3.6}$$

where $G^*(\mu)$ is the conjugate transpose of $G(\mu)$. $\hat{x}^{du}(\mu) := Wz^{du}(\mu)$ is the approximate solution to the dual system, $x^{du}(\mu) \approx \hat{x}^{du}(\mu)$.

Let $r^{pr}(\mu) = B(\mu) - G(\mu)\hat{x}(\mu)$ be the residual of $\hat{x}(\mu)$, and $r^{du}(\mu) = -C(\mu)^* - G^*(\mu)\hat{x}^{du}(\mu)$ be the residual of $\hat{x}^{du}(\mu)$. In order to make the final description of the error bound as concise as possible, we use the representations of r^{pr} and r^{du} in terms of another basis in $\mathbb{C}^n$. Since $\tilde{A}$ is positive definite, its column vectors are a basis in $\mathbb{C}^n$. Therefore, r^{pr} and r^{du} can be represented by the column vectors of $\tilde{A}$, *i.e.*

$$r^{pr}(\mu) = \tilde{A}\xi^{pr}(\mu) \tag{3.7}$$

and

$$r^{du}(\mu) = \tilde{A}\xi^{du}(\mu). \tag{3.8}$$

For the sake of brevity, in the following we will leave out the dependency of $r^{pr}(\mu)$, $r^{du}(\mu)$, $\xi^{pr}(\mu)$, $\xi^{du}(\mu)$, $x(\mu)$, $x^{du}(\mu)$, $\hat{x}(\mu)$, $\hat{x}^{du}(\mu)$, $z(\mu)$, $z^{du}(\mu)$ on μ, which will be clear from the context. We first propose a relation between $H(\mu) - \hat{H}(\mu)$ and the errors of the approximate state vectors $\hat{x}$ and $\hat{x}^{du}$. This relation will be repeatedly used to derive the error bound.

[4]Since we assume that the systems matrices in (2.4)–(2.6) are all real matrices, it is usually preferred that the reduced-order models also have real system matrices. Therefore, we choose real projection matrices $W, V \in \mathbb{R}^{n\times r}$ to guarantee this condition.

Proposition 3.1. *If the reduced-order model* (3.4) *of the primal system and that of the dual system* (3.6) *are obtained by the same pair* W *and* V*, then*

$$H(\mu) - \hat{H}(\mu) = C(\mu)x - C(\mu)\hat{x} = -(\epsilon^{du})^* G(\mu)\epsilon^{pr},$$

where $\epsilon^{du} = x^{du} - \hat{x}^{du}$ *and* $\epsilon^{pr} = x - \hat{x}$.

Proof. From (3.4), we have $W^T B - W^T G(\mu)\hat{x} = 0$, *i.e.*

$$\begin{aligned} & W^T G(\mu)x - W^T G(\mu)\hat{x} = 0 \\ \Leftrightarrow\ & W^T G(\mu)(x - \hat{x}) = 0 \\ \Rightarrow\ & (z^{du})^* W^T G(\mu)(x - \hat{x}) = 0 \\ \Leftrightarrow\ & (\hat{x}^{du})^* G(\mu)(x - \hat{x}) = 0 \\ \Leftrightarrow\ & (\hat{x}^{du})^* G(\mu)\epsilon^{pr} = 0. \end{aligned} \tag{3.9}$$

From (3.5) and (3.9), we get

$$\begin{aligned} C(\mu)x - C(\mu)\hat{x} =& C(\mu)\epsilon^{pr} \\ =& -(x^{du})^*(G^*(\mu))^*\epsilon^{pr} \\ =& -(x^{du})^* G(\mu)\epsilon^{pr} + (\hat{x}^{du})^* G(\mu)\epsilon^{pr}. \\ =& -(\epsilon^{du})^* G(\mu)\epsilon^{pr}. \end{aligned} \tag{3.10}$$

□

Since the computation of ϵ^{du} and ϵ^{pr} involves computation of x^{du} and x, the solutions of the full dual and the full primal systems, $|(\epsilon^{du})^* G(\mu)\epsilon^{pr}|$ cannot act as a computable error bound for $|H(\mu) - \hat{H}(\mu)|$. Next, we will use Proposition 1 and the assumptions on $G(\mu)$ to derive computable error bounds for the real and imaginary parts of $H(\mu) - \hat{H}(\mu)$ separately. The final error bound can be obtained from the error bounds for the real and imaginary parts.

Proposition 3.2. *If the reduced-order model* (3.4) *of the primal system and that of the dual system* (3.6) *are obtained by the same pair* W *and* V*, and* $G(\mu)$ *satisfies* (3.1)*, then*

$$-S_R - \beta_R \le Re(H(\mu) - \hat{H}(\mu)) \le S_R - \beta_R.$$

Here,

$$\beta_R = \frac{1}{4\alpha(\mu)}\left[(\xi^{pr})^*\tilde{A}\xi^{du} + (\xi^{du})^*\tilde{A}\xi^{pr}\right], \qquad S_R = \frac{1}{4\alpha(\mu)}\left[\kappa_0(\xi^{pr})^*\tilde{A}\xi^{pr} + \frac{1}{\kappa_0}(\xi^{du})^*\tilde{A}\xi^{du}\right],$$

and

$$\kappa_0 = \left(\frac{(\xi^{du})^*\tilde{A}\xi^{du}}{(\xi^{pr})^*\tilde{A}\xi^{pr}}\right)^{1/2}.$$

Proof. We begin by defining an auxiliary vector $\epsilon_\alpha^- = \frac{1}{\alpha(\mu)}\xi^{pr} - \frac{1}{\kappa\alpha(\mu)}\xi^{du}$. Here and below, $\kappa > 0$ is a variable to be specified. We first derive an upper bound for $\mathrm{Re}(H(\mu) - \hat{H}(\mu))$. Since $\alpha(\mu) > 0$,

$$\begin{aligned} 0 \le \kappa\alpha(\mu)\left\langle \epsilon^{pr} - \frac{1}{2}\epsilon_\alpha^-, \epsilon^{pr} - \frac{1}{2}\epsilon_\alpha^- \right\rangle &= \kappa\alpha(\mu)\left(\epsilon^{pr} - \frac{1}{2}\epsilon_\alpha^-\right)^* \tilde{A}\left(\epsilon^{pr} - \frac{1}{2}\epsilon_\alpha^-\right) \\ = \kappa\alpha(\mu)(\epsilon^{pr})^*\tilde{A}\epsilon^{pr} + \frac{\kappa\alpha(\mu)}{4}(\epsilon_\alpha^-)^*\tilde{A}\epsilon_\alpha^- - \frac{\kappa\alpha(\mu)}{2}(\epsilon_\alpha^-)^*\tilde{A}\epsilon^{pr} - \frac{\kappa\alpha(\mu)}{2}(\epsilon^{pr})^*\tilde{A}\epsilon_\alpha^- \\ \Leftrightarrow \frac{\kappa\alpha(\mu)}{2}(\epsilon_\alpha^-)^*\tilde{A}\epsilon^{pr} + \frac{\kappa\alpha(\mu)}{2}(\epsilon^{pr})^*\tilde{A}\epsilon_\alpha^- &\le \kappa\alpha(\mu)(\epsilon^{pr})^*\tilde{A}\epsilon^{pr} + \frac{\kappa\alpha(\mu)}{4}(\epsilon_\alpha^-)^*\tilde{A}\epsilon_\alpha^-. \end{aligned} \tag{3.11}$$

From the property of the inner product

$$(\epsilon_\alpha^-)^*\tilde{A}\epsilon^{pr} = \overline{(\epsilon^{pr})^*\tilde{A}\epsilon_\alpha^-}, \tag{3.12}$$

we only have to estimate $(\epsilon^{pr})^*\tilde{A}\epsilon_\alpha^-$ in the last inequality of (3.11). From the definition of ϵ_α^-, and (3.7), (3.8), (3.10), we get

$$\begin{aligned}
(\epsilon^{pr})^*\tilde{A}\epsilon_\alpha^- &= \frac{1}{\alpha(\mu)}(\epsilon^{pr})^*\tilde{A}\xi^{pr} - \frac{1}{\kappa\alpha(\mu)}(\epsilon^{pr})^*\tilde{A}\xi^{du} \\
&= \frac{1}{\alpha(\mu)}(\epsilon^{pr})^*r^{pr} - \frac{1}{\kappa\alpha(\mu)}\overline{(r^{du})^*\epsilon^{pr}} \\
&= \frac{1}{\alpha(\mu)}(\epsilon^{pr})^*(B(\mu) - G(\mu)\hat{x}) - \frac{1}{\kappa\alpha(\mu)}\overline{(-C^*(\mu) - G^*(\mu)\hat{x}^{du})^*\epsilon^{pr}} \\
&= \frac{1}{\alpha(\mu)}(\epsilon^{pr})^*(G(\mu)x - G(\mu)\hat{x}) - \frac{1}{\kappa\alpha(\mu)}\overline{(G^*(\mu)x^{du} - G^*(\mu)\hat{x}^{du})^*\epsilon^{pr}} \\
&= \frac{1}{\alpha(\mu)}(\epsilon^{pr})^*G(\mu)\epsilon^{pr} - \frac{1}{\kappa\alpha(\mu)}\overline{(G^*(\mu)\epsilon^{du})^*\epsilon^{pr}} \\
&= \frac{1}{\alpha(\mu)}(\epsilon^{pr})^*G(\mu)\epsilon^{pr} - \frac{1}{\kappa\alpha(\mu)}\overline{(\epsilon^{du})^*G(\mu)\epsilon^{pr}} \\
&= \frac{1}{\alpha(\mu)}(\epsilon^{pr})^*G(\mu)\epsilon^{pr} + \frac{1}{\kappa\alpha(\mu)}\overline{(C(\mu)x - C(\mu)\hat{x})}.
\end{aligned} \tag{3.13}$$

Using the relation in (3.12), and substituting the last inequality in (3.13) into the last inequality of (3.11) yields

$$\begin{aligned}
&\frac{\kappa\alpha(\mu)}{2}(\epsilon_\alpha^-)^*\tilde{A}\epsilon^{pr} + \frac{\kappa\alpha(\mu)}{2}(\epsilon^{pr})^*\tilde{A}\epsilon_\alpha^- \le \kappa\alpha(\mu)(\epsilon^{pr})^*\tilde{A}\epsilon^{pr} + \frac{\kappa\alpha(\mu)}{4}(\epsilon_\alpha^-)^*\tilde{A}\epsilon_\alpha^- \\
&\Leftrightarrow \frac{\kappa}{2}\left[2\mathrm{Re}((\epsilon^{pr})^*G(\mu)\epsilon^{pr}) + \frac{2}{\kappa}\mathrm{Re}(C(\mu)x - C(\mu)\hat{x})\right] \le \kappa\alpha(\mu)(\epsilon^{pr})^*\tilde{A}\epsilon^{pr} + \frac{\kappa\alpha(\mu)}{4}(\epsilon_\alpha^-)^*\tilde{A}\epsilon_\alpha^- \\
&\Leftrightarrow \kappa\mathrm{Re}((\epsilon^{pr})^*G(\mu)\epsilon^{pr}) + \mathrm{Re}(C(\mu)x - C(\mu)\hat{x}) \le \kappa\alpha(\mu)(\epsilon^{pr})^*\tilde{A}\epsilon^{pr} + \frac{\kappa\alpha(\mu)}{4}(\epsilon_\alpha^-)^*\tilde{A}\epsilon_\alpha^- \\
&\Leftrightarrow \mathrm{Re}(C(\mu)x - C(\mu)\hat{x}) \le -\kappa\mathrm{Re}((\epsilon^{pr})^*G(\mu)\epsilon^{pr}) + \kappa\alpha(\mu)(\epsilon^{pr})^*\tilde{A}\epsilon^{pr} + \frac{\kappa\alpha(\mu)}{4}(\epsilon_\alpha^-)^*\tilde{A}\epsilon_\alpha^- \\
&\Rightarrow \mathrm{Re}(C(\mu)x - C(\mu)\hat{x}) \le \frac{\kappa\alpha(\mu)}{4}(\epsilon_\alpha^-)^*\tilde{A}\epsilon_\alpha^-,
\end{aligned} \tag{3.14}$$

where the last inequality holds due to (3.1). Substituting $\epsilon_\alpha^- = \frac{1}{\alpha(\mu)}\xi^{pr} - \frac{1}{\kappa\alpha(\mu)}\xi^{du}$ into the last inequality of (3.14) gives

$$\begin{aligned}
\mathrm{Re}(C(\mu)x - C(\mu)\hat{x}) &\le \frac{\kappa\alpha(\mu)}{4}(\epsilon_\alpha^-)^*\tilde{A}\epsilon_\alpha^- \\
&\le \frac{\kappa}{4\alpha(\mu)}(\xi^{pr})^*\tilde{A}\xi^{pr} + \frac{1}{4\kappa\alpha(\mu)}(\xi^{du})^*\tilde{A}\xi^{du} - \frac{1}{4\alpha(\mu)}(\xi^{pr})^*\tilde{A}\xi^{du} - \frac{1}{4\alpha(\mu)}(\xi^{du})^*\tilde{A}\xi^{pr} \\
\Leftrightarrow \mathrm{Re}(H(\mu) - \hat{H}(\mu)) &\le f_R(\kappa) - \beta_R,
\end{aligned} \tag{3.15}$$

where $f_R(\kappa) = \frac{\kappa}{4\alpha(\mu)}(\xi^{pr})^*\tilde{A}\xi^{pr} + \frac{1}{4\kappa\alpha(\mu)}(\xi^{du})^*\tilde{A}\xi^{du}$.

Next we derive the lower bound, $\mathrm{Re}(H(\mu) - \hat{H}(\mu)) \ge -f_R(\kappa) - \beta_R$. We now define a second auxiliary vector $\epsilon_\alpha^+ = \frac{1}{\alpha(\mu)}\xi^{pr} + \frac{1}{\kappa\alpha(\mu)}\xi^{du}$. Replacing ϵ_α^- in (3.11) with ϵ_α^+, we obtain a similar expression for ϵ_α^+,

$$\frac{\kappa\alpha(\mu)}{2}(\epsilon_\alpha^+)^*\tilde{A}\epsilon^{pr} + \frac{\kappa\alpha(\mu)}{2}(\epsilon^{pr})^*\tilde{A}\epsilon_\alpha^+ \le \kappa\alpha(\mu)(\epsilon^{pr})^*\tilde{A}\epsilon^{pr} + \frac{\kappa\alpha(\mu)}{4}(\epsilon_\alpha^+)^*\tilde{A}\epsilon_\alpha^+. \tag{3.16}$$

It is not difficult to see from (3.13) that

$$(\epsilon^{pr})^*\tilde{A}\epsilon_\alpha^+ = \frac{1}{\alpha(\mu)}(\epsilon^{pr})^*G(\mu)\epsilon^{pr} - \frac{1}{\kappa\alpha(\mu)}\overline{(C(\mu)x - C(\mu)\hat{x})}. \tag{3.17}$$

Using the relation $(\epsilon_\alpha^+)^*\tilde{A}\epsilon^{pr} = \overline{(\epsilon^{pr})^*\tilde{A}\epsilon_\alpha^+}$, substituting (3.17) into (3.16), and following calculations similar to (3.14), yields

$$\begin{aligned} &\frac{\kappa\alpha(\mu)}{2}(\epsilon_\alpha^+)^*\tilde{A}\epsilon^{pr} + \frac{\kappa\alpha(\mu)}{2}(\epsilon^{pr})^*\tilde{A}\epsilon_\alpha^+ \le \kappa\alpha(\mu)(\epsilon^{pr})^*\tilde{A}\epsilon^{pr} + \frac{\kappa\alpha(\mu)}{4}(\epsilon_\alpha^+)^*\tilde{A}\epsilon_\alpha^+ \\ &\Rightarrow -\mathrm{Re}(C(\mu)x - C(\mu)\hat{x}) \le \frac{\kappa\alpha(\mu)}{4}(\epsilon_\alpha^+)^*\tilde{A}\epsilon_\alpha^+. \end{aligned} \tag{3.18}$$

Substituting $\epsilon_\alpha^+ = \frac{1}{\alpha(\mu)}\xi^{pr} + \frac{1}{\kappa\alpha(\mu)}\xi^{du}$ into the last inequality of (3.18), and following calculations analogous to (3.15), we can assert that

$$\begin{aligned} &-\mathrm{Re}(C(\mu)x - C(\mu)\hat{x}) \le \frac{\kappa\alpha(\mu)}{4}(\epsilon_\alpha^+)^*\tilde{A}\epsilon_\alpha^+ \\ &\Leftrightarrow \mathrm{Re}(H(\mu) - \hat{H}(\mu)) \ge -f_R(\kappa) - \beta_R. \end{aligned} \tag{3.19}$$

Combining the last equality of (3.15) with that of (3.19), we have $|\mathrm{Re}(H(\mu) - \hat{H}(\mu)) + \beta_R| \le f_R(\kappa)$. It is not difficult to check that when $\kappa = \kappa_0$, $f_R(\kappa)$ reaches the minimum, and $f_R(\kappa_0) = S_R$. □

Proposition 3.3. *If the reduced-order model* (3.4) *of the primal system and that of the dual system* (3.6) *are obtained by the same pair* W, V, *and* $G(\mu)$ *satisfies* (3.2), *then*

$$-S_I + \beta_I \le Im(H(\mu) - \hat{H}(\mu)) \le S_I + \beta_I.$$

Here,

$$\beta_I = \frac{1}{4\gamma(\mu)}\left[(\xi^{pr})^*\tilde{A}\xi^{du} + (\xi^{du})^*\tilde{A}\xi^{pr}\right], \qquad S_I = \frac{1}{4\gamma(\mu)}\left[\kappa_0(\xi^{pr})^*\tilde{A}\xi^{pr} + \frac{1}{\kappa_0}(\xi^{du})^*\tilde{A}\xi^{du}\right],$$

and κ_0 *is defined as in Proposition* 3.2.

Proof. We first derive the upper bound for $\mathrm{Im}(H(\mu) - \hat{H}(\mu))$. Similar to the proof of Proposition 2, let us define an auxiliary vector $\epsilon_\gamma^- = \frac{1}{\gamma(\mu)}\xi^{pr} - \frac{1}{\kappa\gamma(\mu)}\xi^{du}$. In the following discussions, $\jmath = \sqrt{-1}$ is the imaginary unit. Since $\gamma(\mu) > 0$,

$$\begin{aligned} 0 &\le \kappa\gamma(\mu)\left\langle \epsilon^{pr} + \frac{\jmath}{2}\epsilon_\gamma^-, \epsilon^{pr} + \frac{\jmath}{2}\epsilon_\gamma^-\right\rangle = \kappa\gamma(\mu)(\epsilon^{pr} + \frac{\jmath}{2}\epsilon_\gamma^-)^*\tilde{A}\left(\epsilon^{pr} + \frac{\jmath}{2}\epsilon_\gamma^-\right) \\ &= \kappa\gamma(\mu)(\epsilon^{pr})^*\tilde{A}\epsilon^{pr} + \frac{\kappa\gamma(\mu)}{4}(\epsilon_\gamma^-)^*\tilde{A}\epsilon_\gamma^- - \frac{\jmath\kappa\gamma(\mu)}{2}(\epsilon_\gamma^-)^*\tilde{A}\epsilon^{pr} + \frac{\jmath\kappa\gamma(\mu)}{2}(\epsilon^{pr})^*\tilde{A}\epsilon_\gamma^- \\ &\Leftrightarrow \frac{\jmath\kappa\gamma(\mu)}{2}(\epsilon_\gamma^-)^*\tilde{A}\epsilon^{pr} - \frac{\jmath\kappa\gamma(\mu)}{2}(\epsilon^{pr})^*\tilde{A}\epsilon_\gamma^- \le \kappa\gamma(\mu)(\epsilon^{pr})^*\tilde{A}\epsilon^{pr} + \frac{\kappa\gamma(\mu)}{4}(\epsilon_\gamma^-)^*\tilde{A}\epsilon_\gamma^-. \end{aligned} \tag{3.20}$$

Since the only difference between ϵ_α^- and ϵ_γ^- is the denominator, from (3.13) we see

$$(\epsilon^{pr})^*\tilde{A}\epsilon_\gamma^- = \frac{1}{\gamma(\mu)}(\epsilon^{pr})^*G(\mu)\epsilon^{pr} + \frac{1}{\kappa\gamma(\mu)}\overline{(C(\mu)x - C(\mu)\hat{x})}. \tag{3.21}$$

We proceed analogously to the proof of Proposition 3.2. Using the relation $(\epsilon_\gamma^-)^*\tilde{A}\epsilon^{pr} = \overline{(\epsilon^{pr})^*\tilde{A}\epsilon_\gamma^-}$, and substituting (3.21) into the last inequality of (3.20), yields

$$\begin{aligned}
&\frac{\jmath\kappa\gamma(\mu)}{2}(\epsilon_\gamma^-)^*\tilde{A}\epsilon^{pr} - \frac{\jmath\kappa\gamma(\mu)}{2}(\epsilon^{pr})^*\tilde{A}\epsilon_\gamma^- \le \kappa\gamma(\mu)(\epsilon^{pr})^*\tilde{A}\epsilon^{pr} + \frac{\kappa\gamma(\mu)}{4}(\epsilon_\gamma^-)^*\tilde{A}\epsilon_\gamma^- \\
&\Leftrightarrow \frac{\jmath^2\kappa}{2}\left[-2\mathrm{Im}((\epsilon^{pr})^*G(\mu)\epsilon^{pr}) + \frac{2}{\kappa}\mathrm{Im}(C(\mu)x - C(\mu)\hat{x})\right] \le \kappa\gamma(\mu)(\epsilon^{pr})^*\tilde{A}\epsilon^{pr} + \frac{\kappa\gamma(\mu)}{4}(\epsilon_\gamma^-)^*\tilde{A}\epsilon_\gamma^- \\
&\Leftrightarrow \kappa\mathrm{Im}((\epsilon^{pr})^*G(\mu)\epsilon^{pr}) - \mathrm{Im}(C(\mu)x - C(\mu)\hat{x}) \le \kappa\gamma(\mu)(\epsilon^{pr})^*\tilde{A}\epsilon^{pr} + \frac{\kappa\gamma(\mu)}{4}(\epsilon_\gamma^-)^*\tilde{A}\epsilon_\gamma^- \\
&\Leftrightarrow -\mathrm{Im}(C(\mu)x - C(\mu)\hat{x}) \le -\kappa\mathrm{Im}(\epsilon^{pr})^*G(\mu)\epsilon^{pr}) + \kappa\gamma(\mu)(\epsilon^{pr})^*\tilde{A}\epsilon^{pr} + \frac{\kappa\gamma(\mu)}{4}(\epsilon_\gamma^-)^*\tilde{A}\epsilon_\gamma^- \\
&\Rightarrow -\mathrm{Im}(C(\mu)x - C(\mu)\tilde{x}) \le \frac{\kappa\gamma(\mu)}{4}(\epsilon_\gamma^-)^*\tilde{A}\epsilon_\gamma^-,
\end{aligned} \tag{3.22}$$

where the last inequality holds because of (3.2). Substituting $\epsilon_\gamma^- = \frac{1}{\gamma(\mu)}\xi^{pr} - \frac{1}{\kappa\gamma(\mu)}\xi^{du}$ into the last inequality of (3.22), and following calculations similar to (3.15) gives

$$\mathrm{Im}(H(\mu) - \hat{H}(\mu)) \ge -f_I(\kappa) + \beta_I, \tag{3.23}$$

where $f_I(\kappa) = \frac{\kappa}{4\gamma(\mu)}(\xi^{pr})^*\tilde{A}\xi^{pr} + \frac{1}{4\kappa\gamma(\mu)}(\xi^{du})^*\tilde{A}\xi^{du}$.

We continue to prove the next claim $\mathrm{Im}(H(\mu) - \hat{H}(\mu)) \le f_I(\kappa) + \beta_I$. Defining a second auxiliary vector $\epsilon_\gamma^+ = \frac{1}{\gamma(\mu)}\xi^{pr} + \frac{1}{\kappa\gamma(\mu)}\xi^{du}$ yields

$$\begin{aligned}
&0 \le \kappa\gamma(\mu)\left\langle \epsilon^{pr} + \frac{\jmath}{2}\epsilon_\gamma^+, \epsilon^{pr} + \frac{\jmath}{2}\epsilon_\gamma^+\right\rangle = \kappa\gamma(\mu)(\epsilon^{pr} + \frac{\jmath}{2}\epsilon_\gamma^+)^*\tilde{A}\left(\epsilon^{pr} + \frac{\jmath}{2}\epsilon_\gamma^+\right) \\
&\Leftrightarrow \frac{\jmath\kappa\gamma(\mu)}{2}(\epsilon_\gamma^+)^*\tilde{A}\epsilon^{pr} - \frac{\jmath\kappa\gamma(\mu)}{2}(\epsilon^{pr})^*\tilde{A}\epsilon_\gamma^+ \le \kappa\gamma(\mu)(\epsilon^{pr})^*\tilde{A}\epsilon^{pr} + \frac{\kappa\gamma(\mu)}{4}(\epsilon_\gamma^+)^*\tilde{A}\epsilon_\gamma^+.
\end{aligned} \tag{3.24}$$

From (3.21), we know

$$(\epsilon^{pr})^*\tilde{A}\epsilon_\gamma^+ = \frac{1}{\gamma(\mu)}(\epsilon^{pr})^*G(\mu)\epsilon^{pr} - \frac{1}{\kappa\gamma(\mu)}\overline{(C(\mu)x - C(\mu)\hat{x})}. \tag{3.25}$$

Using the relation $(\epsilon_\gamma^+)^*\tilde{A}\epsilon^{pr} = \overline{(\epsilon^{pr})^*\tilde{A}\epsilon_\gamma^+}$, substituting (3.25) into the last inequality of (3.24), and following (3.22), we obtain

$$\mathrm{Im}(C(\mu)x - C(\mu)\tilde{x}) \le \tfrac{\kappa\gamma(\mu)}{4}(\epsilon_\gamma^+)^*\tilde{A}\epsilon_\gamma^+. \tag{3.26}$$

Substituting $\epsilon_\gamma^+ = \frac{1}{\gamma(\mu)}\xi^{pr} + \frac{1}{\kappa\gamma(\mu)}\xi^{du}$ into (3.26), it follows immediately

$$\mathrm{Im}(H(\mu) - \hat{H}(\mu)) \le f_I(\kappa) + \beta_I. \tag{3.27}$$

From (3.23) and (3.27), we have $|\mathrm{Im}(H(\mu) - \hat{H}(\mu)) - \beta_I| \le f_I(\kappa)$. When $\kappa = \kappa_0$, $\min_\kappa f_I(\kappa) = f_I(\kappa_0) = S_I$. □

Based on Proposition 3.2 and 3.3, we can immediately get the error bound for $|H(\mu) - \hat{H}(\mu)|$ given in the following theorem.

Theorem 3.4. *The error of $\hat{H}(\mu)$ is bounded by $\Delta(\mu)$ defined as below:*

$$|H(\mu) - \hat{H}(\mu)| = \sqrt{|Re(H(\mu) - \hat{H}(\mu))|^2 + |Im(H(\mu) - \hat{H}(\mu))|^2} \le \sqrt{B_R^2 + B_I^2} := \Delta(\mu). \tag{3.28}$$

Here, $B_R = \max\{|S_R - \beta_R|, |-S_R - \beta_R|\}$ and $B_I = \max\{|-S_I + \beta_I|, |S_I + \beta_I|\}$.

3.2. Error bound for MIMO systems

For MIMO systems, the transfer function $H(\mu)$ is a matrix. The ikth entry $H_{ik}(\mu)$ corresponds to a SISO system, whose input is $u_k(t)$, the kth entry of the input vector $u(t)$, and whose output is $y_i(t) = C(\mu)(i,:)x(t)$, the ith entry of the output response $y(t)$. The transfer function $\hat{H}(\mu)$ of the reduced-order model is also a matrix. The ikth entry $\hat{H}_{ik}(\mu)$ is an approximation of $H_{ik}(\mu)$ for the corresponding SISO system. Therefore, the error between $\hat{H}_{ik}(\mu)$ and $H_{ik}(\mu)$ can be measured by $\Delta_{ik}(\mu)$, which can be computed from (3.28) as

$$|H_{ik}(\mu) - \hat{H}_{ik}(\mu)| \leq \sqrt{(B_R^{ik})^2 + (B_I^{ik})^2} =: \Delta_{ik}(\mu),$$

To compute B_R^{ik}, B_I^{ik} corresponding to $\Delta_{ik}(\mu)$, the output matrix $C(\mu)$ should be replaced by $C(\mu)(i,:)$, the ith row in $C(\mu)$. The input matrix $B(\mu)$ should be replaced by $B(\mu)(:,k)$, the kth column in $B(\mu)$, $\forall 1 \leq i \leq m_1$, $1 \leq k \leq m_2$.

Once all $\Delta_{ik}(\mu)$, $1 \leq i \leq m_1, 1 \leq k \leq m_2$ are computed by (3.28), the final error bound can be taken as the maximum of them, *i.e.*

$$||H(\mu) - \hat{H}(\mu)||_{\max} = \max_{ik} |H_{ik}(\mu) - \hat{H}_{ik}(\mu)| \leq \max_{ik} \Delta_{ik}(\mu). \tag{3.29}$$

In the next section, we propose an *a posteriori* error bound for $\hat{H}(\mu)$, which does not require the coercivity assumption on the real part and the imaginary part of $G(\mu)$, respectively. Instead, only an inf-sup condition suffices, which implies the error bound is valid for more general LTI systems.

4. Error bound for general LTI systems

In this section, we derive an error bound for more general LTI systems. Instead of (3.1) and (3.2), the matrix-valued function $G(\mu)$ is assumed to satisfy an *inf-sup condition* of the following form[5]:

$$\inf_{\substack{w\in\mathbb{C}^n \\ w\neq 0}} \sup_{\substack{v\in\mathbb{C}^n \\ v\neq 0}} \frac{w^* G(\mu) v}{||w||_2 ||v||_2} = \beta(\mu) > 0, \mathrm{Re}(s) \geq 0, \forall \tilde{\mu} \in \mathcal{D} \subset \mathbb{R}^{\tilde{p}}. \tag{4.1}$$

We still rely on the primal system in (3.3) and the dual system in (3.5). The reduced-order model for the primal system is of the same form as the system in (3.4). The reduced-order model for the dual system can be constructed more flexibly as

$$\begin{aligned} (W^{du})^T G^*(\mu) V^{du} z^{du}(\mu) &= -(W^{du})^T C^*(\mu), \\ \hat{y}^{du}(\mu) &= B^*(\mu) V^{du} z^{du}(\mu), \end{aligned} \tag{4.2}$$

where W^{du} and V^{du} can be different from V and W for the primal system, that means it is allowed that $W^{du} \neq V$ and $V^{du} \neq W$.

Again, we define two auxiliary variables $e(\mu) = (\hat{x}^{du})^* r^{pr}$ and $\tilde{y}(\mu) = C(\mu)\hat{x} - e(\mu)$. Here $\hat{x}^{du} = V^{du} z^{du}$ is the approximate solution to (3.5).

Theorem 4.1. *For a SISO LTI system, if $G(\mu)$ satisfies (4.1), then $|y(\mu) - \tilde{y}(\mu)| \leq \tilde{\Delta}_g(\mu)$, $\tilde{\Delta}_g(\mu) := \frac{||r^{du}||_2 ||r^{pr}||_2}{\beta(\mu)}$. As a result, $|H(\mu) - \hat{H}(\mu)| = |C(\mu)x - C(\mu)\hat{x}| \leq \Delta_g(\mu)$, $\Delta_g(\mu) := \tilde{\Delta}_g(\mu) + |e(\mu)|$.*

[5]Same as before, the entries of the vector μ are functions of the parameters $\tilde{\mu}$ and the Laplace variable s, *i.e.* $\mu_i := \phi_i(\tilde{\mu}_1, \ldots, \tilde{\mu}_{\tilde{p}}, s)$, as defined in (4). Here we also restrict s to be on the closed right half plane: $\mathrm{Re}(s) \geq 0, \forall \tilde{\mu} \in \mathcal{D} \subset \mathbb{R}^{\tilde{p}}$, to avoid defining $G(\mu)$ on the system eigenvalues (See footnote 3).

Proof. The dual system $G^*(\mu)x^{du} = -C^*(\mu)$ implies that

$$(x - \hat{x})^* G^*(\mu) x^{du} = -(x - \hat{x})^* C^*(\mu). \tag{4.3}$$

From the definition of the residual $r^{pr} = B(\mu) - G(\mu)\hat{x} = G(\mu)(x - \hat{x})$ for the primal system, we get

$$(x^{du})^* r^{pr} = (x^{du})^* G(\mu)(x - \hat{x}). \tag{4.4}$$

Combining (4.3) with (4.4), it is obvious that

$$-C(\mu)(x - \hat{x}) = (x^{du})^* r^{pr}.$$

Then

$$\begin{aligned} |y(\mu) - \tilde{y}(\mu)| &= |C(\mu)x - C(\mu)\hat{x} + (\hat{x}^{du})^* r^{pr}| \\ &= |-(x^{du})^* r^{pr} + (\hat{x}^{du})^* r^{pr}| \\ &= |-(x^{du} - \hat{x}^{du})^* r^{pr}| \\ &\leq ||(x^{du} - \hat{x}^{du})||_2 ||r^{pr}||_2. \end{aligned} \tag{4.5}$$

Replacing w in (4.1) with $x^{du} - \hat{x}^{du}$ yields

$$\sup_{v \in \mathbb{C}^n} \frac{(x^{du} - \hat{x}^{du})^* G(\mu) v}{||x^{du} - \hat{x}^{du}||_2 ||v||_2} \geq \beta(\mu),$$

i.e.

$$\sup_{v \in \mathbb{C}^n} \frac{(x^{du} - \hat{x}^{du})^* G(\mu) v}{||v||_2} \geq \beta(\mu) ||x^{du} - \hat{x}^{du}||_2. \tag{4.6}$$

Since

$$\frac{(x^{du} - \hat{x}^{du})^* G(\mu) v}{||v||_2} \leq \frac{||G^*(\mu)(x^{du} - \hat{x}^{du})||_2 ||v||_2}{||v||_2} = ||G^*(\mu)(x^{du} - \hat{x}^{du})||_2,$$

and with the choice $v = v_0 = G^*(\mu)(x^{du} - \hat{x}^{du})$,

$$\frac{(x^{du} - \hat{x}^{du})^* G(\mu) v_0}{||v_0||_2} = ||G^*(\mu)(x^{du} - \hat{x}^{du})||_2,$$

it suffices to make the following observation:

$$\sup_{v \in \mathbb{C}^n} \frac{(x^{du} - \hat{x}^{du})^* G^*(\mu) v}{||v||_2} = ||G^*(\mu)(x^{du} - \hat{x}^{du})||_2. \tag{4.7}$$

Combining (4.6) with (4.7) shows that

$$||G^*(\mu)(x^{du} - \hat{x}^{du})||_2 \geq \beta(\mu) ||x^{du} - \hat{x}^{du}||_2.$$

From the definition of $r^{du} = -C^*(\mu) - G^*(\mu)\hat{x}^{du} = G^*(\mu)x^{du} - G^*(\mu)\hat{x}^{du}$, we get

$$||r^{du}||_2 \geq \beta(\mu) ||x^{du} - \hat{x}^{du}||_2. \tag{4.8}$$

Substituting (4.8) into (4.5) we obtain

$$|y(\mu) - \tilde{y}(\mu)| \leq \frac{||r^{du}||_2 ||r^{pr}||_2}{\beta(\mu)}.$$

Since $\tilde{y}(\mu) = C(\mu)\hat{x} - e(\mu)$,

$$|C(\mu)x - C(\mu)\hat{x}| - |e(\mu)| \le |y(\mu) - \tilde{y}(\mu)| \le \frac{||r^{du}||_2||r^{pr}||_2}{\beta(\mu)}.$$

Finally,

$$|H(\mu) - \hat{H}(\mu)| = |C(\mu)x - C(\mu)\hat{x}| \le \frac{||r^{du}||_2||r^{pr}||_2}{\beta(\mu)} + |e(\mu)| =: \Delta_g(\mu). \qquad \square$$

Remark 4.2. For MIMO systems, we can use a similar technique as in Section 3.2 to get the final error bound for the reduced transfer matrix.

Remark 4.3. If $W^{du} = V$, and $V^{du} = W$, and $W^T G(\mu)V$ is invertible on the imaginary axis, then $e(\mu) = 0$, since

$$\begin{aligned} e(\mu) &= (\hat{x}^{du})^* r^{pr} \\ &= (V^{du} z^{du})^* (B - G(\mu)Vz) \\ &= (Wz^{du})^* (B - G(\mu)Vz) \\ &= (z^{du})^* W^T [B - G(\mu)V(W^T G(\mu)V)^{-1} W^T B] \\ &= (z^{du})^* [W^T B - W^T G(\mu)V(W^T G(\mu)V)^{-1} W^T B] \\ &= 0. \end{aligned} \tag{4.9}$$

In this case, the error bound reduces to

$$|H(\mu) - \hat{H}(\mu)| \le \frac{||r^{du}||_2||r^{pr}||_2}{\beta(\mu)},$$

and it can actually be straightforwardly derived based on the error analysis in [23] (see Sect. 5.2 in Chap. 5). The above assumption on $W^T G(\mu)V$ is reasonable, since in systems theory, we usually assume that no poles of the transfer function are purely imaginary. As the error is usually measured on the imaginary axis (frequency response), a ROM with eigenvalues on the imaginary axis would be a poor approximation with infinite error. Thus, we may assume the ROM to be invertible on the imaginary axis without loss of generality.

Although the matrix pair $W^{du} = V$, $V^{du} = W$ implies $|e(\mu)| = 0$, they are not always the optimal choice for the dual system in the sense of making the residual r^{du} as small as possible. As a result, the error bound which is also influenced by r^{du} decreases probably much slower than using an optimal W^{du}, V^{du}, possibly different from W, V. In this situation, although no contribution of $|e(\mu)| = 0$ to the error bound, the contribution of r^{du} is much bigger. Take the dual system in (3.5) for a non-parametric LTI system as an example. If only Galerkin projection is used to get the reduced-order model, *i.e.*, $W = V$, then based on the idea of model order reduction and moment-matching MOR (see Sect. 7.1.1), the subspace $\mathcal{V}^{du}$ which includes the trajectory of x^{du} in the frequency domain should be $\mathcal{V}^{du} = \mathcal{K}_{q+1}((\tilde{E}_c(s_0)), \tilde{C}(s_0))$ as defined in (7.2), so that range$(V^{du}) = \mathcal{K}_{q+1}((\tilde{E}_c(s_0)), \tilde{C}(s_0))$ is the proper choice for the projection matrix V^{du}, rather than $V^{du} = W = V = \mathcal{K}_{q+1}(\tilde{E}_b(s_0), \tilde{B}(s_0))$ defined in (7.1). Simulation results in Section 8 also support our analysis. However, if Petrov−Galerkin projection is used to obtain the reduced-order model, the choice $W^{du} = V$ and $V^{du} = W$ is optimal for moment-matching MOR.

Remark 4.4. Note that, for non-parametric systems, $\mu = s$. In the following, we use $\Delta_g(s)$ to denote the error bound $\Delta_g(\mu)$ for non-parametric systems.

Remark 4.5. For the error bound $\Delta(\mu)$ proposed in Section 3, a global W which is independent of the parameter μ, is needed in order to prove Proposition 1. For the error bound derivation in Proposition 2 and Proposition 3, W, V do not appear in the proofs, no requirement on the global property of W, V is needed.

For the error bound $\Delta_g(\mu)$ proposed in Section 4, the three main ingredients for computing the error bound are the two residuals and $\beta(\mu)$. For any PMOR method, regardless of the choice of global W, V or local W, V [3], the finally derived reduced-order model is global, which means the two residuals should be available, even if the reduced-order models of the primal system and the dual system are not in the form of (3.4) and (4.2), respectively. What we only need is the solution of the reduced-order models of the primal and the dual systems, from which we can compute the residuals. Therefore (3.4) and (4.2) can be written in a more general form:

$$\begin{aligned}\hat{G}(\mu)z(\mu) &= \hat{B}(\mu),\\ \hat{y}(\mu) &= \hat{C}(\mu)z(\mu),\\ \hat{G}_{du}(\mu)z^{du}(\mu) &= \hat{C}_{du}(\mu),\\ \hat{y}^{du}(\mu) &= \hat{B}_{du}(\mu)z^{du}(\mu),\end{aligned}$$

Those reduced-order models are obtained not necessarily using the projection framework in (3.4), (4.2) with global W, V, instead, they can be obtained by, *e.g.* matrix interpolation using local W, Vs [3]. The error bound $\Delta_g(\mu)$ is still valid for such reduced-order models. However, to be consistent throughout the paper, we prefer to use the projection framework in (3.4), (4.2).

5. Computation of the error bounds

5.1. Computation of $\Delta(\mu)$

In Section 3.1, the error bound $\Delta(\mu)$ is derived for special LTI systems, where the matrix $G(\mu)$ is required to satisfy the two coercive assumptions (3.1) and (3.2). $\Delta(\mu)$ is determined by the two vectors ξ^{pr} and ξ^{du}, and the two variables $\alpha(\mu)$ and $\gamma(\mu)$.

5.1.1. Computation of $\alpha(\mu)$ and $\gamma(\mu)$

For parameterized LTI systems, to compute $\alpha(\mu)$ and $\gamma(\mu)$, we have to compute $\mathrm{Re}(x^*G(\mu)x)$ and $\mathrm{Im}(x^*G(\mu)x)$. It is easy to see that if $G(\mu)$ has no special form, $\mathrm{Re}(x^*G(\mu)x)$ and $\mathrm{Im}(x^*G(\mu)x)$ are almost impossible to be computed. Therefore, we assume that $G(\mu)$ is in the affine form,

$$G(\mu) = E_0 + E_1\mu_1 + \ldots + E_p\mu_p. \tag{5.1}$$

Even with this assumption, it is still not easy to identify $\mathrm{Re}(x^*G(\mu)x)$ or $\mathrm{Im}(x^*G(\mu)x)$ from $x^*G(\mu)x$, if one has no insight into the structure of the vector μ of parameters. For a general vector $\mu \in \mathbb{R}^p$, it is hard to compute $\mathrm{Re}(x^*G(\mu)x)$ or $\mathrm{Im}(x^*G(\mu)x)$. However, for some special μ, it is possible. For example, if $\mu = (s, \tilde{\mu})^T$, where $\tilde{\mu} \in \mathbb{R}$ is the only geometrical or physical parameter. Such a μ could come from a parametrized first-order LTI system (2.4) with only one parameter $\tilde{\mu}$ associated with the matrix A, so that $G(\mu) = sE - \tilde{\mu}A$.

In the following, we assume that A and E are symmetric and $G(\mu) = sE - \tilde{\mu}A$, then for any $s = \sigma_0 + \jmath\omega$,

$$\begin{aligned}\frac{\mathrm{Re}(x^*G(\mu)x)}{x^*\tilde{A}x} &= \frac{\mathrm{Re}(x^*(\jmath\omega E + \sigma_0 E - \tilde{\mu}A)x)}{x^*\tilde{A}x}\\ &= \frac{x^*\bar{A}(\tilde{\mu})x}{x^*\tilde{A}x}\\ &= \frac{\tilde{x}^*(R^{-1})^*\bar{A}(\tilde{\mu})R^{-1}\tilde{x}}{\tilde{x}^*\tilde{x}}\\ &\geq \lambda_{\min}((R^{-1})^*\bar{A}(\tilde{\mu})R^{-1}) := \alpha(\mu),\end{aligned}$$

where $\bar{A}(\tilde{\mu}) = \sigma_0 E - \tilde{\mu} A$, $R^* R = \tilde{A}$ is the Cholesky factorization of $\tilde{A}$, and $\tilde{x} = Rx$. $\lambda_{\min}((R^{-1})^* \bar{A} R^{-1})$ is the smallest eigenvalue of $(R^{-1})^* \bar{A} R^{-1}$. If A and E are symmetric, $x^* \bar{A}(\tilde{\mu}) x$ is the real part of $x^* G(\mu) x$. Therefore, from the property of the Rayleigh quotient, we can take $\alpha(\mu)$ as the smallest eigenvalue of the symmetric matrix $(R^{-1})^* \bar{A}(\tilde{\mu}) R^{-1}$. As a result, $\bar{A}$ needs to be positive definite to guarantee that $\alpha(\mu) > 0$. If $\tilde{A} = I$, the identity matrix, then $\alpha(\mu)$ simplifies to the minimal eigenvalue of the matrix $\bar{A}(\tilde{\mu})$. Taking use of the special form of $\bar{A}(\tilde{\mu}) = \sigma_0 E - \tilde{\mu} A$, we can see that $(R^{-1})^* \bar{A}(\tilde{\mu}) R^{-1} = \sigma_0 (R^{-1})^* E R^{-1} - \tilde{\mu} (R^{-1})^* A R^{-1}$. Here, both $(R^{-1})^* E R^{-1}$ and $(R^{-1})^* A R^{-1}$ can be precomputed independently of $\tilde{\mu}$. In any case, smallest eigenvalue of the symmetric matrix $(R^{-1})^* \bar{A}(\tilde{\mu}) R^{-1}$ must be computed for each value of $\tilde{\mu}$.

Remark 5.1. For first-order LTI systems (2.4), one choice of $\tilde{A}$ might be $\tilde{A} = s_0 E - \tilde{\mu}_0 A$, where s_0 and $\tilde{\mu}_0$ are chosen so that $\tilde{A}$ is symmetric positive definite. In the non-parametric case, where $\tilde{\mu}$ disappears, $\tilde{A} = s_0 E - A$ and $\bar{A} = \sigma_0 E - A$. Then if $\sigma_0 = s_0$, we obtain the simple case $\alpha(s) = 1$. Often, $s = \jmath\omega$, and $\sigma_0 = 0$, then we can use $\tilde{A} = -A$ to define the norm, if A is symmetric negative definite. In this situation, $\bar{A} = -A$ too, so that $\alpha(s) \equiv 1$.

For the estimation of $\gamma(\mu)$ with $G(\mu) = sE - \tilde{\mu} A$, we have

$$\begin{aligned} \frac{\mathrm{Im}(x^* G(\mu) x)}{x^* \tilde{A} x} &= \frac{\omega x^* E x}{x^* \tilde{A} x} \\ &= \frac{\omega \tilde{x}^* (R^{-1})^* E R^{-1} \tilde{x}}{\tilde{x}^* \tilde{x}} \\ &\geq \omega \lambda_{\min}((R^{-1})^* E R^{-1}) := \gamma(\mu), \end{aligned}$$

$\lambda_{\min}((R^{-1})^* E R^{-1})$ is the smallest eigenvalue of $(R^{-1})^* E R^{-1}$. Since it is assumed that $\gamma(\mu) > 0$, E must be symmetric positive definite. Since $\bar{A} = \bar{A}^T$ needs to be positive definite, it implicates that $\sigma_0 \geq 0$, $\tilde{\mu} \geq 0$ and $A = A^T < 0$. This means that the error bound is valid for frequencies on the closed right half plane: $\mathrm{Re}(s) \geq 0$ and for nonnegative parameter $\tilde{\mu} \geq 0$.

In summary,

- for non-parametrized first-order LTI systems (2.4), once we have computed the smallest eigenvalue of $(R^{-1})^* \bar{A} R^{-1}$ ($\bar{A} = \sigma_0 E - A$), we have obtained $\alpha(s)$. Furthermore, $\lambda_{\min}((R^{-1})^* E R^{-1})$ can be computed *a priori*. Thus, for each value of s, $\gamma(s)$ is equal to $\lambda_{\min}((R^{-1})^* E R^{-1})$ multiplied by ω. That means, the two eigenvalue problems are solved only once, and can be computed independently of s. The computation of the smallest eigenvalue of a positive definite matrix can be cheaply computed using the Lanczos process which requires only a small number of sparse matrix-vector multiplications. Note that when the real part of s changes, *i.e.* when σ_0 changes, $\alpha(s)$ has to be nevertheless recomputed. This rarely happens, since we are often interested in the frequency response, where $\sigma_0 = 0$.
- If the system is in second-order form (2.5), but is non-parametric, successful computation of $\alpha(s)$ and $\gamma(s)$ will depend on the properties (*e.g.*, symmetry, positive definiteness) of all the three system matrices E, K, A. The analysis is similar to that for the first-order LTI systems.
- However, for parametrized LTI system, even with the simplest case $G(\mu) = sE - \tilde{\mu} A$, $\alpha(\mu)$ has to be recomputed whenever $\tilde{\mu}$ varies. For more general parametrized LTI systems (2.4)(2.5), where both $E(\mu)$ and $A(\mu)$ are parameter-dependent, it is almost impossible to compute $\alpha(\mu)$ and $\gamma(\mu)$.
- As a conclusion, the error bound $\Delta(\mu)$ is particularly efficient for non-parametrized first-order LTI systems (2.4) with E symmetric positive definite and A symmetric negative definite.

5.1.2. Computation of ξ^{pr} and ξ^{du}

Next, we show how to efficiently compute the two vectors ξ^{pr} and ξ^{du}. Since $\tilde{A}$ is assumed to be positive definite, ξ^{pr} is uniquely determined by: $\xi^{pr} = \tilde{A}^{-1} r^{pr}$. Similarly from (3.8), ξ^{du} can be uniquely determined by $\xi^{du} = \tilde{A}^{-1} r^{du}$.

The two vectors ξ^{pr} and ξ^{du} are functions of μ. For each value of μ, two full-size linear systems must be solved to get ξ^{pr}, and ξ^{du}, which looks expensive. However, some μ-independent terms in $\tilde{A}^{-1}r^{pr}$ or $\tilde{A}^{-1}r^{du}$ can be precomputed. For example, for a non-parametrized first-order LTI system, $G(\mu) = sE - A$, so that

$$\begin{aligned}
\xi^{pr}(s) &= \tilde{A}^{-1}r^{pr}(s),\\
&= \tilde{A}^{-1}(B - sEVz + AVz),\\
&= \tilde{A}^{-1}[B - sEV(sW^TEV - W^TAV)^{-1}W^TB+\\
&\quad AV(sW^TEV - W^TAV)^{-1}W^TB],\\
&= \tilde{A}^{-1}B - s\tilde{A}^{-1}EV(sW^TEV - W^TAV)^{-1}W^TB\\
&\quad +\tilde{A}^{-1}AV(sW^TEV - W^TAV)^{-1}W^TB.
\end{aligned}$$

The terms W^TEV, W^TAV, W^TB need to be computed only once, and can be repeatedly used for any value of s. Although $(sW^TEV - W^TAV)$ needs to be factored for each possible value of s, this is done in the reduced state-space, which is therefore quite cheap. The matrix V usually has few columns, therefore, the terms $\tilde{A}^{-1}EV$, $\tilde{A}^{-1}AV$, $\tilde{A}^{-1}B$ can be computed by solving $2r + m_1$ linear systems. Here, r is the number of the columns in V, which is also the size of the reduced-order model, and m_1 is the number of columns in B. As a result, the estimation of ξ^{pr} at any fixed value of s can be done efficiently. Likewise, ξ^{du} can be computed by following a similar strategy. Furthermore, when the standard 2-norm is used, $\tilde{A}$ reduces to the identity matrix. Then there is no need to solve linear systems.

5.2. Computation of $\Delta_g(\mu)$

The key for computing $\Delta_g(\mu)$ is how to compute $\beta(\mu)$. The condition (4.1) is equivalent to

$$\inf_{w\in\mathbb{C}^n}\frac{1}{||w||_2}\sup_{v\in\mathbb{C}^n}\frac{w^*G(\mu)v}{||v||_2} = \beta(\mu). \tag{5.2}$$

On the one hand,

$$\frac{w^*G(\mu)v}{||v||_2} \le \frac{||G^*(\mu)w||_2||v||_2}{||v||_2} = ||G^*(\mu)w||_2.$$

On the other hand, when $v = G^*(\mu)w$,

$$\frac{w^*G(\mu)v}{||v||_2} = ||G^*(\mu)w||_2.$$

Therefore,

$$\sup_{v\in\mathbb{C}^n}\frac{w^*G(\mu)v}{||v||_2} = ||G^*(\mu)w||_2.$$

Substituting this into (5.2), we get

$$\inf_{w\in\mathbb{C}^n}\frac{||G^*(\mu)w||_2}{||w||_2} = \beta(\mu).$$

From the Courant-Fischer theorem, we obtain,

$$\min_{w\in\mathbb{C}^n}\frac{w^*G(\mu)G^*(\mu)w}{w^*w} = \lambda_{\min}(G(\mu)G^*(\mu)),$$

i.e. $\beta(\mu) = \sqrt{\lambda_{\min}(G(\mu)G^*(\mu))}$. The error bound $\Delta_g(\mu)$ includes the two residuals r^{pr} and r^{du}. For the computation of r^{pr} and r^{du}, the affinity Assumption (5.1) on $G(\mu)$ is preferred. With the affine form, it is not difficult to see that r^{pr} and r^{du} can be efficiently computed [28].

Remark 5.2. Clearly, for each value of μ, the minimal eigenvalue of $G(\mu)G^*(\mu)$, or equivalently, the minimal singular value of $G(\mu)$, must be computed to get $\beta(\mu)$. It is impractical if $\beta(\mu)$ must be estimated at many samples of μ. The method proposed in [31] can be used to compute a lower bound $\beta_{LB}(\mu)$ of $\beta(\mu)$, such that $\beta_{LB}(\mu)$ could be computed efficiently through solving a sequence of small optimization problems. Without solving any large-scale problems, $\beta_{LB}(\mu)$ is expected to be quickly available for each sample of μ. However, since it is a lower bound of $\beta(\mu)$, $\Delta_g(\mu)$ computed by $\beta_{LB}(\mu)$ would over estimate the real error of the reduced transfer function $\hat{H}(\mu)$. It is observed that when the range of μ is very large, β_{LB} is not close to $\beta(\mu)$ at all. Furthermore, the accuracy of $\beta_{LB}(\mu)$ highly relies on the optimization solvers, which cannot guarantee to converge to an optimal solution for each sample of μ. The method in [31] becomes complicated for parametrized systems, and may easily lead to a meaningless lower bound $\beta_{LB}(\mu)$. More efficient methods for computing or estimating $\beta(\mu)$ will be future work.

Remark 5.3. As compared with $\Delta(\mu)$, no strict limitation on the systems matrices $E(\mu)$, $A(\mu)$, such as symmetry, positive definiteness, is required. Therefore, $\Delta_g(\mu)$ is valid for more general LTI systems.

6. Reformulated reduced-order model with tighter error bounds

It is discussed in Section 4 that except for some special cases, the value of $|e(\mu)|$ in the error bound is nonzero in general. Motivated by the analysis in [2], we show in this section that a different reduced-order model can be constructed from $\tilde{y}(\mu)$ in Theorem 4.1, so that $e(\mu)$ in the error bounds disappears.

From the definition of $e(\mu) = (\hat{x}^{du})^* r^{pr}(\mu)$ and $r^{pr} = B(\mu) - G(\mu)V(W^TG(\mu)V)^{-1}W^TB(\mu)$, $\hat{x}^{du} = V^{du}z^{du} = -V^{du}[(W^{du})^TG^*(\mu)V^{du}]^{-1}(W^{du})^TC^*(\mu)$, we observe

$$
\begin{aligned}
& y(\mu) - \tilde{y}(\mu) \\
&= C(\mu)x - C(\mu)\hat{x} + (\hat{x}^{du})^* r^{pr} \\
&= C(\mu)x - C(\mu)\hat{x} - C(\mu)(W^{du})[(V^{du})^TG(\mu)W^{du}]^{-1}(V^{du})^T[B(\mu) - G(\mu)V(W^TG(\mu)V)^{-1}W^TB(\mu)] \\
&= C(\mu)G^{-1}(\mu)B(\mu) - C(\mu)V(W^TG(\mu)V)^{-1}W^TB(\mu) - \\
&\quad C(\mu)W^{du}[(V^{du})^TG(\mu)W^{du}]^{-1}(V^{du})^T[B(\mu) - G(\mu)V(W^TG(\mu)V)^{-1}W^TB(\mu)] \\
&= C(\mu)G^{-1}(\mu)B(\mu) - C(\mu)V(W^TG(\mu)V)^{-1}W^TB(\mu) - C(\mu)W^{du}[(V^{du})^TG(\mu)W^{du}]^{-1}(V^{du})^TB(\mu) \\
&\quad -C(\mu)W^{du}[(V^{du})^TG(\mu)W^{du}]^{-1}(V^{du})^TG(\mu)V(W^TG(\mu)V)^{-1}W^TB(\mu).
\end{aligned}
\tag{6.1}
$$

The right-hand side of the last equality in (6.1) can be written in matrix form as below,

$$
\underbrace{C(\mu)G^{-1}(\mu)B(\mu)}_{H(\mu)} - \underbrace{\begin{bmatrix} C(\mu)V & C(\mu)W^{du} \end{bmatrix} \begin{bmatrix} W^TG(\mu)V & 0 \\ (V^{du})^TG(\mu)V & (V^{du})^TG(\mu)W^{du} \end{bmatrix}^{-1} \begin{bmatrix} W^TB(\mu) \\ (V^{du})^TB(\mu) \end{bmatrix}}_{\tilde{H}(\mu)}.
$$

Clearly, $y(\mu) = H(\mu)$ and $\tilde{y}(\mu) = \tilde{H}(\mu)$. Using $\tilde{H}(\mu)$ to approximate $H(\mu)$, the error bound for $\tilde{H}(\mu)$ is $\tilde{\Delta}_g(\mu)$, *i.e.* $|H(\mu) - \tilde{H}(\mu)| \leq \tilde{\Delta}_g(\mu)$. There is no additional term $|e(\mu)|$ in the error bound.

Next we consider constructing a reduced-order model whose transfer function is $\tilde{H}(\mu)$. From $\tilde{H}(\mu)$, the corresponding system with zero initial condition[6], can be written as

$$\begin{aligned}\begin{bmatrix} W^T G(\mu) V & 0 \\ (V^{du})^T G(\mu) V & (V^{du})^T G(\mu) W^{du} \end{bmatrix} \begin{bmatrix} z_1 \\ z_2 \end{bmatrix} &= \begin{bmatrix} W^T B(\mu) \\ (V^{du})^T B(\mu) \end{bmatrix} u_{\mathcal{L}}(s), \\ y &= \begin{bmatrix} C(\mu) V & C(\mu) W^{du} \end{bmatrix} \begin{bmatrix} z_1 \\ z_2 \end{bmatrix}\end{aligned} \tag{6.2}$$

in frequency (Laplace) domain. Here and below, $u_{\mathcal{L}}(\cdot)$ is the Laplace transform of the input signal $u(t)$.

If the parametrized LTI system in (2.4) or (2.5) is considered, then $G(\mu)$ can be written as $G(\mu) = sE(\tilde{\mu}) - A(\tilde{\mu})$ or $G(\mu) = s^2 M(\tilde{\mu}) + sK(\tilde{\mu}) + A(\tilde{\mu})$. Inserting, *e.g.* $G(\mu) = sE(\tilde{\mu}) - A(\tilde{\mu})$, $B(\mu) = B(\tilde{\mu})$, $C(\mu) = C(\tilde{\mu})$ from (2.4) into (6.2), we get

$$\begin{aligned}\begin{bmatrix} s\hat{E}_{11}(\tilde{\mu}) - \hat{A}_{11}(\tilde{\mu}) & 0 \\ s\hat{E}_{21}(\tilde{\mu}) - \hat{A}_{21}(\tilde{\mu}) & s\hat{E}_{22}(\tilde{\mu}) - \hat{A}_{22}(\tilde{\mu}) \end{bmatrix} \begin{bmatrix} z_1 \\ z_2 \end{bmatrix} &= \begin{bmatrix} W^T B(\tilde{\mu}) \\ (V^{du})^T B(\tilde{\mu}) \end{bmatrix} u_{\mathcal{L}}(s), \\ y &= \begin{bmatrix} C(\tilde{\mu}) V & C(\tilde{\mu}) W^{du} \end{bmatrix} \begin{bmatrix} z_1 \\ z_2 \end{bmatrix},\end{aligned}$$

where $\hat{E}_{11}(\tilde{\mu}) = W^T E(\tilde{\mu}) V$, $\hat{A}_{11}(\tilde{\mu}) = W^T A(\tilde{\mu}) V$, $\hat{E}_{21} = (V^{du})^T E(\tilde{\mu}) V$, $\hat{A}_{21}(\tilde{\mu}) = (V^{du})^T A(\tilde{\mu}) V$, $\hat{E}_{22}(\tilde{\mu}) = (V^{du})^T E(\tilde{\mu}) W^{du}$, $\hat{A}_{22}(\tilde{\mu}) = (V^{du})^T A(\tilde{\mu}) W^{du}$.

Using inverse Laplace transform, the reduced-order model in time domain is

$$\begin{aligned}\begin{bmatrix} \hat{E}_{11}(\tilde{\mu}) & 0 \\ \hat{E}_{21}(\tilde{\mu}) & \hat{E}_{22}(\tilde{\mu}) \end{bmatrix} \begin{bmatrix} \dot{z}_1(t) \\ \dot{z}_2(t) \end{bmatrix} &= \begin{bmatrix} \hat{A}_{11}(\tilde{\mu}) & 0 \\ \hat{A}_{21}(\tilde{\mu}) & \hat{A}_{22}(\tilde{\mu}) \end{bmatrix} \begin{bmatrix} z_1(t) \\ z_2(t) \end{bmatrix} + \begin{bmatrix} W^T B(\tilde{\mu}) \\ (V^{du})^T B(\tilde{\mu}) \end{bmatrix} u(t), \\ \hat{y} &= \begin{bmatrix} C(\tilde{\mu}) V & C(\tilde{\mu}) W^{du} \end{bmatrix} \begin{bmatrix} z_1(t) \\ z_2(t) \end{bmatrix}.\end{aligned} \tag{6.3}$$

It shows that for the original system in (2.4), a reduced-order model as in (6.3) can be derived, whose transfer function is $\tilde{H}(s)$, satisfying $|H(\mu) - \tilde{H}(\mu)| \leq \tilde{\Delta}_g(\mu)$. For the second-order parametrized system in (2.5), the corresponding reduced-order model can also be obtained in a similar way. Notice also that the reduced-order model (6.3) cannot be obtained by means of an explicit Petrov–Galerkin projection applied to the original system in (2.4). Instead, the projection

$$\tilde{W} = \begin{bmatrix} W & \\ & V^{du} \end{bmatrix} \tilde{V} = \begin{bmatrix} V & \\ & W^{du} \end{bmatrix}$$

is applied to a non-minimal realization of the original system, namely

$$\begin{aligned}\begin{bmatrix} E_(\tilde{\mu}) & 0 \\ E(\tilde{\mu}) & E(\tilde{\mu}) \end{bmatrix} \begin{bmatrix} \dot{x}_1(t) \\ \dot{x}_2(t) \end{bmatrix} &= \begin{bmatrix} A(\tilde{\mu}) & 0 \\ A(\tilde{\mu}) & A(\tilde{\mu}) \end{bmatrix} \begin{bmatrix} x_1(t) \\ x_2(t) \end{bmatrix} + \begin{bmatrix} B(\tilde{\mu}) \\ B(\tilde{\mu}) \end{bmatrix} u(t), \\ y &= \begin{bmatrix} C(\tilde{\mu}) & C(\tilde{\mu}) \end{bmatrix} \begin{bmatrix} x_1(t) \\ x_2(t) \end{bmatrix}.\end{aligned}$$

[6]Here, we assume that the original system (*e.g.* (2.4) or (2.5)) has zero initial condition. For a system with nonzero initial condition, one can use coordinate transformation $\tilde{x} = x - x(0)$ to get a transformed system with state vector $\tilde{x}$, and with zero initial condition $\tilde{x}(0) = 0$. A reduced-order model with zero initial condition can be obtained by applying MOR to the transformed system [17].

In summary, there are two reduced-order models available for the original system in (2.4), one is the reduced-order model,

$$\begin{aligned} W^T E(\tilde{\mu}) V \frac{\mathrm{d}z}{\mathrm{d}t} &= W^T A(\tilde{\mu}) V z + W^T B(\tilde{\mu}) u(t), \\ \hat{y}(t,\tilde{\mu}) &= C V(\tilde{\mu}) z, \end{aligned} \tag{6.4}$$

constructed directly from the original system; the other is the reformulated reduced-order model in (6.3). On the one hand, if using the same stopping criteria $\varepsilon_{\mathrm{tol}}$ in Algorithm 2, the reduced-order model in (6.4) is usually less accurate than the one in (6.3) (though both satisfy the error tolerance $\varepsilon_{\mathrm{tol}}$), because the error bound $\Delta_g(\mu)$ for $\hat{H}(\mu)$ is less sharp than $\tilde{\Delta}_g(\mu)$ for $\tilde{H}(\mu)$. On the other hand, the reduced-order model in (6.3) could be of much bigger size than the one in (6.4). From this point of view, the reduced-order model in (6.4) is practically preferable, since it is of much smaller size and also satisfies an acceptable error tolerance. The analysis is aided by an example in Section 8.

7. Automatic generation of the reduced-order models

We explore algorithms of automatic constructing reliable reduced-order models in this section. In particular, we show that the moment-matching MOR methods can be adaptively implemented using the proposed error bounds. To this end, we first present a brief review of the MOR methods, and point out the necessity of adaptively implementing the methods.

7.1. Review of moment-matching MOR methods

7.1.1. Moment-matching MOR for non-parametrized LTI systems

For moment-matching methods, the matrices W, V are constructed from the transfer function (matrix) $H(s)$. Taking the system (2.4) as an example. If it is non-parametric, then the system matrices are all $\tilde{\mu}$-independent, so that $H(s)$ can be expanded into a power series about an expansion point s_0 as

$$\begin{aligned} H(s) &= C[(s - s_0 + s_0)E - A]^{-1} B \\ &= C[(s - s_0)E + (s_0 E - A)]^{-1} B \\ &= C[I + (s_0 E - A)^{-1} E(s - s_0)]^{-1} (s_0 E - A)^{-1} B \\ &= \sum_{i=0}^{\infty} \underbrace{C[-(s_0 E - A)^{-1} E]^i (s_0 E - A)^{-1} B}_{:= m_i(s_0)} (s - s_0)^i, \end{aligned}$$

then $m_i(s_0)$, $i = 0, 1, 2, \ldots$ are called the ith order moments of the transfer function. The columns of V span the Krylov subspace

$$\mathrm{range}\{V\} = \mathcal{K}_{q+1}(\tilde{E}_b(s_0), \tilde{B}(s_0)) := \mathrm{span}\left\{\tilde{B}(s_0), \ldots, (\tilde{E}_b(s_0))^q \tilde{B}(s_0)\right\}, \tag{7.1}$$

where $\tilde{E}_b(s_0) = (s_0 E - A)^{-1} E$, $\tilde{B}(s_0) = (s_0 E - A)^{-1} B$. The columns of W span the Krylov subspace

$$\mathrm{range}\{W\} = \mathcal{K}_{q+1}(\tilde{E}_c(s_0), \tilde{C}(s_0)) := \mathrm{span}\left\{\tilde{C}(s_0), \ldots, (\tilde{E}_c(s_0))^q \tilde{C}(s_0)\right\}, \tag{7.2}$$

where $\tilde{C}(s_0) = (s_0 E - A)^{-T} C^T$, $\tilde{E}_c(s_0) = (s_0 E - A)^{-T} E^T$. Obviously, W and V span two Krylov subspaces. It is proved in [23], that the transfer function of the reduced-order model $\hat{H}(s)$ matches the first $2q + 1$ moments of the original transfer function $H(s)$. It is obvious that the accuracy of the reduced-order model depends on the expansion point s_0. In many cases, only a single expansion point is insufficient to attain the required accuracy. Multiple-point expansion is preferred such that the large error caused at frequencies far away from the

expansion point can be reduced. A reduced-order model of better accuracy and smaller order can be obtained by multiple-point expansion. Therefore proper selection of multiple expansion points is important. Previous studies on multiple-point expansion are found in [1,12,13,20,26,29]. In [26], the expansion points are chosen such that the reduced-order model is locally optimal. A binary search is used in [1, 12, 20] for adaptive, but heuristic selection of the expansion points. In Section 7.2, we readdress the problem of selecting multiple expansion points by using the global *a posteriori* error bounds proposed in Section 3 and Section 4.

7.1.2. Review of multi-moment matching PMOR methods

Multi-moment matching PMOR methods can be found in [11,16,18,19,44,45]. All these methods are based on Galerkin projection, *i.e.* $W = V$. In this section, the robust PMOR method from [11,19] is reviewed. The method applies to the systems in (2.4) (2.5) or (2.6). It depends on series expansion of the state x in the frequency (Laplace) domain. Note that for the steady system with algebraic equations (2.6), direct series expansion of x in (2.6) suffices. Assume in the frequency domain,

$$x = G^{-1}(\mu)B(\mu)u_{\mathcal{L}}(\mu),$$

with $G(\mu)$ being of the affine formulation in (5.1). Then given an expansion point $\mu^0 = [\mu_1^0, \mu_2^0, \cdots, \mu_p^0]$, x can be expanded as

$$\begin{aligned} x &= [I - (\sigma_1 M_1 + \ldots + \sigma_p M_p)]^{-1}\tilde{B}_M u_{\mathcal{L}}(\mu) \\ &= \sum_{i=0}^{\infty}(\sigma_1 M_1 + \ldots + \sigma_p M_p)^i \tilde{B}_M u_{\mathcal{L}}(\mu), \end{aligned}$$

where $\tilde{B}_M(\mu) = [G(\mu^0)]^{-1}B(\mu)$, $M_i = -[G(\mu^0)]^{-1}E_i$, $i = 1, 2, \ldots, p$, and $\sigma_i = \mu_i - \mu_i^0$, $i = 1, 2, \ldots, p$. We call the coefficients in the above series expansion the moment matrices of the parametrized system. The corresponding multi-moments of the transfer function are those moment matrices multiplied by $C(\mu)$ from the left.

To get the projection matrix V, instead of directly computing the moment matrices [16], a numerically robust method is proposed in [11, 19]. The method combines the recursions in (7.3) below, with a repeated modified Gram−Schmidt process so that the moment matrices are computed implicitly.

$$\begin{aligned} &R_0 = B_M,\ R_1 = [M_1 R_0, \ldots, M_p R_0], \\ &R_2 = [M_1 R_1, \ldots, M_p R_1], \\ &\vdots, \\ &R_q = [M_1 R_{q-1}, \ldots, M_p R_{q-1}], \\ &\vdots, \end{aligned} \tag{7.3}$$

where $B_M = \tilde{B}_M$, if $B(\mu)$ dose not depend on μ. Otherwise, $B_M = [\tilde{B}_{M1}, \ldots, \tilde{B}_{Mp}]$, if $B(\mu)$ can be approximated by an affine form, *e.g.*, $B(\mu) \approx B_1\mu_1 + \ldots + B_p\mu_p$. Here $\tilde{B}_{Mi} = [G(\mu^0)]^{-1}B_i$, $i = 1, \ldots, p$. The computed $V = V_{\mu^0}$ is an orthonormal basis of the subspace spanned by the moment matrices,

$$\text{range}\{V_{\mu^0}\} = \text{span}\{R_0, R_1, \ldots, R_q\}_{\mu^0}, \tag{7.4}$$

and depends on the expansion point μ^0. The accuracy of the reduced-order model can be improved by increasing the number of terms in (7.4), whereby more multi-moments can be matched.

It is noticed that the dimension of R_j increases exponentially. If the number p of parameters in a parametrized system is larger than 2, it is advantageous to use multiple point expansion, such that only the low order moment matrices, *e.g.* R_j, $j \leq 2$, have to be computed for each expansion point. As a result, the order of the reduced-order model can be kept small. Given a group of expansion points μ^i, $i = 0, \ldots, m$, a matrix V_{μ^i} can be computed from (7.4) for each μ^i as

$$\text{range}\{V_{\mu^i}\} = \text{span}\{R_0, R_1, \ldots, R_q\}_{\mu^i}.$$

The final projection matrix V is a combination (orthogonalization) of all the matrices V_{μ^i},

$$V = \text{orth}\{V_{\mu^0}, \ldots, V_{\mu^m}\}. \tag{7.5}$$

Here, selecting the expansion points μ^i is unavoidable. Algorithm 2 is proposed in Section 7.2 for adaptively selecting the expansion points μ^i using the *a posteriori* error bound $\Delta_g(\mu)$ from Section 4.

7.2. Algorithms for automatic generation of reduced-order models

The algorithms in this section follow the idea of the greedy algorithm widely used in the reduced basis community. A large sample space Ξ_{train} of the variable s or the vector of parameters μ, covering the whole interesting frequency/parameter domain, must be initially given. During each step of the algorithm, a point $\hat{s}$ or $\hat{\mu}$ in Ξ_{train}, which causes the largest error (indicated by the error bound $\Delta(s)$, $\Delta_g(s)$ or $\Delta_g(\mu)$), is chosen as the next expansion point. The process continues until the largest error among all the samples in Ξ_{train} is smaller than an acceptable error tolerance ε_{tol} for the reduced-order model.

Algorithm 1. Automatic generation of the reduced-order model by adaptively selecting expansion points $\hat{s}$ for non-parametrized LTI systems.

Require: Initial expansion point: $\hat{s}$; Ξ_{train}: a large set of samples of s, taken over the interesting frequency range.
Ensure: V, W.
1: $W = []; V = []$;
2: Set $\varepsilon (> \varepsilon_{\text{tol}})$;
3: **while** $\varepsilon > \varepsilon_{\text{tol}}$ **do**
4: $\quad \text{range}(V_{\hat{s}}) = \mathcal{K}_{q+1}(\tilde{E}_b(\hat{s}), \tilde{B}(\hat{s}))$;
5: $\quad \text{range}(W_{\hat{s}}) = \mathcal{K}_{q+1}(\tilde{E}_c(\hat{s}), \tilde{C}(\hat{s}))$;
6: $\quad V = \text{orth}\{V, V_{\hat{s}}\}$; $W^{du} = V$;
7: $\quad W = \text{orth}\{W, W_{\hat{s}}\}$; $V^{du} = W$;
8: $\quad \hat{s} = \arg \max_{s \in \Xi_{\text{train}}} \Delta(s)$ (or $\Delta_g(s)$);
9: $\quad \varepsilon = \Delta(\hat{s})$ or $(\Delta_g(\hat{s}))$;
10: **end while**.

Remark 7.1. Petrov–Galerkin projection with $W \neq V$ is used in Algorithm 1. One can certainly use only V to get the reduced-order model, which reduces to the Galerkin projection method in [38]. It is discussed in [38] that by using the Galerkin projection, the reduced-order model preserves the passivity of the original system, which is an important property in circuit simulation. To compute the error bound $\Delta_g(s)$, W^{du}, V^{du} are needed. In the algorithm, we use $W^{du} = V$ and $V^{du} = W$, such that the second part $|e(s)|$ in the error bound reduces to zero. However, as is discussed at the end of Section 4, if for Galerkin projection where only one projection matrix V^{du} is needed for the dual system, it is preferred to use

$$\text{range}(V_{\hat{s}}^{du}) = \mathcal{K}_{q+1}((\tilde{E}_c(\hat{s})), \tilde{C}(\hat{s})), \tag{7.6}$$

for a chosen expansion point $\hat{s}$, rather than $V^{du} = V$, *i.e.* V^{du} should be computed based on the trajectory of the state x^{du} of the dual system.

In the following, we consider an algorithm for parametrized LTI systems. Since the multi-moment matching PMOR method in Section 7.1.2 is a Galerkin projection method. We use also Galerkin projection in the

algorithm, though the algorithm can be straightforwardly extended to any other Petrov−Galerkin methods. From (7.5), we see that the reduced-order model depends on the expansion points $\mu_i, i = 0, \ldots, m$. Algorithm 2 adaptively chooses the multiple expansion points, which cause the largest errors at the subsequent iteration steps. The next expansion point $\hat{\mu} = (\hat{\mu}_1, \ldots, \hat{\mu}_p)$ is chosen as the point at which the current reduced transfer function $\hat{H}(\mu)$ has the biggest error measured by the error bound $\Delta_g(\mu)$. The projection matrices for the dual system at a particular expansion point $\hat{\mu}$ are chosen as $W_{\hat{\mu}}^{du} = V_{\hat{\mu}}^{du} = \text{span}\{R_0^{du}, \ldots, R_q^{du}\}_{\hat{\mu}}$, where $R_0^{du}, \ldots, R_q^{du}$ are composed of the moment matrices of the dual system, and are defined analogously as for $R_0, \ldots, R_q$ in (7.3). In particular, $R_j^{du} = [M_1^{du} R_{j-1}, \ldots, M_p^{du} R_{j-1}]$, $j = 1, \ldots, q$. $R_0^{du} = [G^*(\hat{\mu})]^{-1}(-C^*(\mu))$, and $M_i^{du} = [G^*(\hat{\mu})]^{-1} E_i^T$, $i = 1, \ldots, p$.

Algorithm 2. Automatic generation of the reduced-order model by adaptively selecting expansion points $\hat{\mu}$ for parametrized LTI systems.

Require: Initial expansion point: $\hat{\mu}$; Ξ_{train}: a large set of samples of μ, taken over the interesting range of all the parameters $\mu_1, \ldots, \mu_p$.
Ensure: V, W.
1: $W = []; V = []$;
2: Set $\varepsilon (> \varepsilon_{\text{tol}})$;
3: **while** $\varepsilon > \varepsilon_{\text{tol}}$ **do**
4: $\quad V_{\hat{\mu}} = \text{span}\{R_0, \ldots, R_q\}_{\hat{\mu}}$;
5: $\quad V = \text{orth}\{V, V_{\hat{\mu}}\}$; $W = V$;
6: $\quad V_{\hat{\mu}}^{du} = \text{span}\{R_0^{du}, \ldots, R_q^{du}\}_{\hat{\mu}}$;
7: $\quad V^{du} = \text{orth}\{V^{du}, V_{\hat{\mu}}^{du}\}$; $W^{du} = V^{du}$;
8: $\quad \hat{\mu} = \arg \max_{\mu \in \Xi_{\text{train}}} \Delta_g(\mu)$;
9: $\quad \varepsilon = \Delta_g(\hat{\mu})$;
10: **end while**.

Remark 7.2. Note that the dimension of the training set Ξ_{train} in Algorithm 2 may grow exponentially with the number p of the parameters in $\mu \in \mathbb{R}^p$ if the tensor product sampling approach is used. However, one can use sparse grids or other adaptive sampling techniques [15,27,47] to avoid the exponential growth. Nevertheless, suffering from curse of dimensionality is a common problem with almost all PMOR methods and algorithms. Furthermore, the error of the reduced-order model computed by Algorithm 1 and Algorithm 2 cannot be guaranteed to be below ε_{tol} everywhere in the frequency/parameter domain, but just at the samples of the frequency/parameters in Ξ_{train}, at which the error bound is evaluated.

8. Simulation results

In this section, we use four examples exhibiting different properties to show the performance of the error bounds. Three of them are non-parametrized LTI systems. The last example is a parametrized LTI system with four parameters. We use Galerkin projection $W = V$ to get the reduced-order models for all the examples. Note that in the following, complex samples of s are included in Ξ_{train} of Algorithm 1 and Algorithm 2, leading to a complex V. To obtain real reduced-order matrices, we use $V = \{\text{Re}(V), \text{Im}(V)\}$ to transform V into a real matrix.

When computing $\Delta_g(s)$, the projection matrix V^{du} for the dual system is computed by (7.6). When computing $\Delta(s)$, we take $\tilde{A} = I$, such that the norm $||\cdot||_{\tilde{A}}$ reduces to the standard 2-norm. In this case, the two coefficient vectors ξ^{pr}, ξ^{du} equal to the two residuals, therefore, there is no need to solve the two linear systems in Section 5.1.2.

The error bounds derived in the above sections are designed for the absolute error, *e.g.* $\varepsilon^{ab}(\mu) = |H(\mu) - \hat{H}(\mu)|$ for a SISO system. In the following results, we also show the performance of the error bound for the relative

TABLE 1. Spiral inductor, $\varepsilon_{\text{tol}} = 10^{-3}$, $n = 1434$, $r = 24$.

Iteration	$\hat{s}/(2\pi\jmath)$	$\varepsilon^{\text{re}}_{\max}$	$\Delta^{\text{re}}(\hat{s})$
1	1	0.23	1.86×10^{4}
2	1×10^{10}	0.04	2.85×10^{3}
3	4×10^{7}	6.6×10^{-5}	0.3
4	3.89×10^{8}	4×10^{-8}	3.5×10^{-4}

error defined as $\varepsilon^{\text{re}}(\mu) = \varepsilon^{ab}/|H(\mu)|$. Accordingly, $\Delta^{\text{re}}(\mu) = \Delta(\mu)/|\hat{H}(\mu)|$, $\Delta^{\text{re}}_g(\mu) = \Delta_g(\mu)/|\hat{H}(\mu)|$ are used as the error estimates for the relative errors, since $H(\mu)$ is never computed in practice.

For a MIMO system, the true error is firstly defined entry-wise, then the maximum is taken, so that $\varepsilon^{ab}(\mu) = \max_{ij} |H_{ij}(\mu) - \hat{H}_{ij}(\mu)|$ is the absolute true error, and $\varepsilon^{\text{re}}(\mu) = \max_{ij} \frac{|H_{ij}(\mu) - \hat{H}_{ij}(\mu)|}{|H_{ij}(\mu)|}$ is the relative true error, $i = 1, \ldots, m_1, j = 1, \ldots, m_2$. The error bound for the absolute error is already defined in (3.29), $\Delta(\mu) = \max_{ij} \Delta_{ij}(\mu)$. The error bound for the relative error is defined as $\Delta^{\text{re}}(\mu) = \max_{ij} \frac{\Delta_{ij}(\mu)}{|\hat{H}_{ij}(\mu)|}$. The same definitions also apply to $\Delta_g(\mu)$. For both SISO and MIMO systems, when there are no parameters, $\mu = s$ in the error bounds as well as in the true errors.

At each iteration step of Algorithm 1 and Algorithm 2, the maximal error bound in Ξ_{train}, is computed, and is used as the error bound for the reduced-order model. Therefore, the maximal true error $\varepsilon^{ab}_{\max} = \max_{\mu_i \in \Xi} \varepsilon^{ab}(\mu_i)$ or $\varepsilon^{\text{re}}_{\max} = \max_{\mu_i \in \Xi} \varepsilon^{\text{re}}(\mu_i)$ is used for a comparison. In the following, Ξ in the definitions of $\varepsilon^{ab}_{\max}$ or $\varepsilon^{\text{re}}_{\max}$ may refer to Ξ^j_{train} or $\Xi^j_{\text{ver}}, j = 1, 2, 3, 4$. When the error bound for $\tilde{H}(\mu)$ of the reformulated reduced-order model in Section 6 is studied, the corresponding true errors are denoted by $\tilde{\varepsilon}^{ab}_{\max}$ and $\tilde{\varepsilon}^{\text{re}}_{\max}$ respectively.

8.1. Results for $\Delta(s)$

The two non-parametrized LTI systems involved in this subsection are in the form of (2.4), and have symmetric positive definite matrix E and symmetric negative definite matrix A. One is a SISO system, a PEEC model of a spiral inductor. The other is a single-input, multiple-output (SIMO) system, the model of an optical filter. They can be found in the Oberwolfach MOR benchmark Collection[7]. The model of the spiral inductor is of size $n = 1434$, and the size of the optical filter model is $n = 1668$. There are 5 outputs for the filter model. The working frequency range for the spiral inductor is $f \in [0, 10GHz]$, numerically $f \in [0, 10^{10}]$. The optical filter is assumed to work in the range of $f \in [0, 1KHz]$, numerically $f \in [0, 10^3]$. For each example, the variable $s = 2\pi\jmath f$ is sampled in the above frequency interval to form the sample space Ξ_{train} in Algorithm 1.

8.1.1. Example 1: The spiral inductor

For this example, we take the sample space as:

$$\Xi^1_{\text{train}} : \left\{ s_i = 2\pi\jmath f_i, f_i = 10^{(i/100)}, i = 1, \ldots, 1000 \right\}$$

where s_i are the samples in Ξ^1_{train}. The first 6 moments ($q = 5$ in Algorithm 1) are matched for each chosen expansion point $\hat{s}$. The initial expansion point is taken as $\hat{s} = 2\pi\jmath\hat{f} = 2\pi\jmath$, with $\hat{f} = 1$. Three more expansion points are adaptively selected by Algorithm 1. Finally, a reduced-order model of order $r = 24$, and with sufficient accuracy, is derived. The results are listed in Table 1. $\Delta^{\text{re}}(\hat{s})$ in the table is the relative error bound at the selected expansion point $\hat{s}$, which is also the maximal error of the reduced-order model in Ξ^1_{train} estimated by $\Delta^{\text{re}}(s)$. $\varepsilon^{\text{re}}_{\max}$ is the true maximal relative error of the reduced-order model in Ξ^1_{train}, at the current iteration step. The final reduced-order model is obtained at the last iteration step, and this is also the case for the results in all

[7]URL: http://portal.uni-freiburg.de/imteksimulation/downloads/benchmark.

TABLE 2. Spiral inductor, $\varepsilon_{\text{tol}} = 10^{-3}$, $n = 1434$, $r = 24$.

Iteration	$\hat{s}/(2\pi\jmath)$	$\varepsilon^{ab}_{\max}$	$\Delta(\hat{s})$
1	1	0.02	252.8
2	1.4×10^{7}	1.9×10^{-4}	2.42
3	1×10^{10}	3.6×10^{-6}	2.5×10^{-2}
4	1.2×10^{8}	7.5×10^{-9}	9.2×10^{-5}

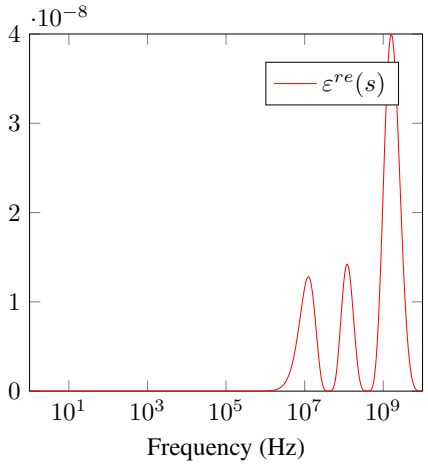

FIGURE 1. Spiral inductor, the true relative error over Ξ^1_{ver}.

the Tables (Figures) below. The data shows that $\Delta^{\text{re}}(s)$ is a bound for the true error of the reduced-order model at all the samples in Ξ^1_{train}. The results for the absolute error are listed in Table 2, where $\Delta(\hat{s})$ has been demonstrated to be a rigorous bound for $\varepsilon^{ab}_{\max}$, the maximal absolute error of the reduced-order model in Ξ^1_{train}.

In Figure 1, we further show that $\Delta^{\text{re}}(s)$ can actually bound the true error $\varepsilon^{\text{re}}(s)$ of the final reduced-order model in the whole frequency range. That means, if we use more densely distributed samples, *e.g.*, 2000 exponentially distributed samples,

$$\Xi^1_{\text{ver}} : \left\{ s_i = 2\pi\jmath f_i, i = 1, \ldots, 2000, f_i = 10^{(i/200)} \right\}$$

to represent the whole interesting frequency interval $[0, 10^{10}]$, the errors of the reduced-order model at those sample points are still smaller than $\Delta^{\text{re}}(\hat{s}) = 3.5 \times 10^{-4}$ at the last iteration step in Table 1, which is the error bound for the final reduced-order model.

Similar results can be given by the absolute error bound $\Delta(s)$, and will not be repeated.

It is interesting to see that the training sample space Ξ_{train} does not have to be too rich. If 2000 samples are taken to form the training space (instead of the previously used 1000 samples in Ξ^1_{train}):

$$\Xi^{\text{rich}_1}_{\text{train}} : \left\{ f_i = 10^{(i/200)}, s_i = 2\pi\jmath f_i, i = 1, \ldots, 2000 \right\},$$

the results in Tables 3 and 4 are the same as those in Tables 1 and 2.

8.1.2. Example 2: The tunable optical filter

The second example is a SIMO system, so the definitions for true errors and the error bounds of the MIMO systems are used.

TABLE 3. Spiral inductor, $\varepsilon_{\text{tol}} = 10^{-3}$, $r = 24$, $\Xi^{\text{rich}_1}_{\text{train}}$.

Iteration	$\hat{s}/(2\pi\jmath)$	$\varepsilon^{\text{re}}_{\max}$	$\Delta^{\text{re}}(\hat{s})$
1	1	0.23	1.86×10^{4}
2	1×10^{10}	0.04	2.85×10^{3}
3	4×10^{7}	6.6×10^{-5}	0.3
4	3.89×10^{8}	4×10^{-8}	3.5×10^{-4}

TABLE 4. Spiral inductor, $\varepsilon_{\text{tol}} = 10^{-3}$, $r = 24$, $\Xi^{\text{rich}_1}_{\text{train}}$.

Iteration	$\hat{s}/(2\pi\jmath)$	$\varepsilon^{ab}_{\max}$	$\Delta(\hat{s})$
1	1	0.02	252.8
2	1.4×10^{7}	1.9×10^{-4}	2.42
3	1×10^{10}	3.6×10^{-6}	2.5×10^{-2}
4	1.2×10^{8}	7.5×10^{-9}	9.2×10^{-5}

TABLE 5. Optical filter, $\varepsilon_{\text{tol}} = 10^{-3}$, $n = 1668$, $r = 12$.

Iteration	$\hat{s}/(2\pi\jmath)$	$\varepsilon^{\text{re}}_{\max}$	$\Delta^{\text{re}}(\hat{s})$
1	1	2.5	3.2×10^{3}
2	966	3.8×10^{-3}	21.1
3	462.4	3.4×10^{-5}	0.17
4	676	4.8×10^{-6}	7.9×10^{-2}
5	188.4	9.3×10^{-8}	8.7×10^{-4}

For this example, we choose 600 sample points in the interesting frequency interval $f \in [0, 10^3]$ to form the sample space,

$$\Xi^{2}_{\text{train}} : \left\{ f_i = 10^{(i/200)}, s_i = 2\pi\jmath f_i, i = 1, \ldots, 600 \right\}.$$

Finally, 121 samples are selected as the expansion points. The reduced-order model is of order $r = 12$. In Algorithm 1, we take $q = 1$, *i.e.* the first 2 moments are matched for each expansion point.

The dashed line in Figure 2a shows the absolute error bound $\Delta(\hat{s})$ at each of the selected expansion points $\hat{s}$, which bounds the true maximal absolute error $\varepsilon^{ab}_{\max}$, plotted by the solid line.

In order to validate the error bound, the true errors $\varepsilon^{ab}(s)$ of the final reduced-order model at more dense sample points are plotted in Figure 2b. There are 2100 exponentially distributed sample points taken in $[0, 10^3]$:

$$\Xi^{2}_{\text{ver}} : \left\{ f_i = 10^{(i/700)}, s_i = 2\pi\sqrt{-1} f_i, i = 1, \ldots, 2100 \right\}.$$

The true error at each sample point is also below the error bound at the final iteration step in Figure 2a.

The results of the relative error bound $\Delta^{\text{re}}(s)$ are presented in Table 5. Here the final reduced-order model with good accuracy is obtained within 5 iteration steps, and 5 expansion points $\hat{s}$ are used.

8.2. Results for $\Delta_g(s)$

We use the model of an interconnect[8] to demonstrate the behavior of $\Delta_g(s)$. The model is a non-parametrized LTI system in (2.4), and is of size $n = 6134$. Since the matrix E is singular, the error bound $\Delta(s)$ is not valid anymore. The interesting frequency range is $f \in [0, 3GHz]$, *i.e.* $f \in [0, 3 \times 10^9]$.

[8]The detailed description for the example can be found in [20].

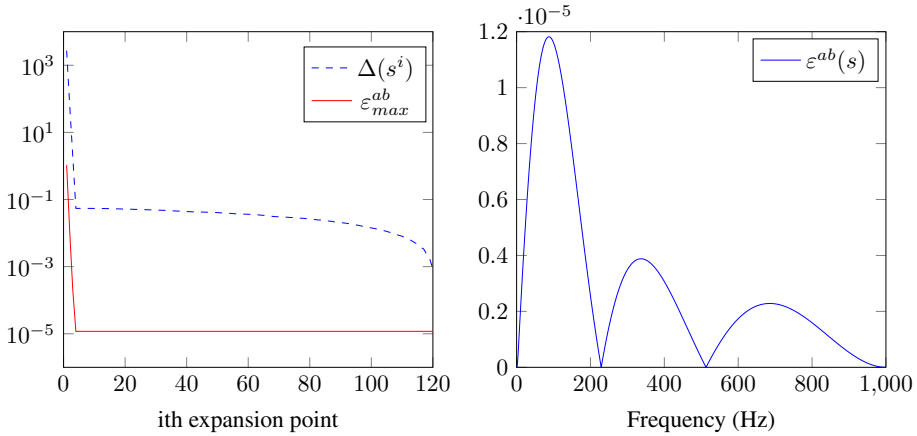

(a) $\Delta(s)$ over Ξ^2_{train} (b) ε^{max}_{true} over Ξ^2_{ver}

FIGURE 2. Optical filter, $q = 1$, $\varepsilon_{\text{tol}} = 10^{-3}$, $n = 1668$, $r = 12$.

TABLE 6. RLC tree, $\varepsilon_{\text{tol}} = 10^{-3}$, $n = 6134$, $r = 24$.

Iteration	$\hat{s}/(2\pi\jmath)$	$\varepsilon^{ab}_{\max}$	$\Delta_g(\hat{s})$
1	0	0.3916	2.93×10^6
2	3.0000×10^9	5.4495×10^{-4}	3.93×10^5
3	1.7665×10^9	4.1075×10^{-8}	31.54
4	1.1146×10^9	4.1076×10^{-8}	3.11
5	2.1733×10^9	4.1073×10^{-8}	0.23
6	2.4385×10^9	4.1070×10^{-8}	3.3×10^{-3}
7	0.3525×10^9	4.1077×10^{-8}	6.64×10^{-8}

TABLE 7. RLC tree, $\varepsilon_{\text{tol}} = 10^{-3}$, $n = 6134$, $r = 26$.

Iteration	$\hat{s}/(2\pi\jmath)$	$\varepsilon^{\text{re}}_{\max}$	$\Delta^{\text{re}}_g(\hat{s})$
1	0	1.25	6.07×10^7
2	2.67×10^9	1.4660×10^{-4}	6.08×10^4
3	1.77×10^9	3.3174×10^{-8}	22.69
4	9.27×10^8	3.3161×10^{-8}	8.23
5	3.00×10^9	8.7115×10^{-10}	1.47
6	1.34×10^9	8.7809×10^{-10}	1.32
7	3.44×10^8	8.6021×10^{-10}	9.70×10^{-6}

A training sample space containing 900 samples,

$$\Xi^3_{\text{train}} : \left\{ f_i = 3 \times 10^{(i/100)}, s_i = 2\pi\jmath f_i, i = 1, \ldots, 900 \right\},$$

is used to compute the expansion points. We take $q = 5$ in Algorithm 1. The simulation results of $\Delta_g(s)$ and of $\Delta^{\text{re}}_g(s)$ are listed in Table 6 and Table 7. A reduced-order model is successfully found by using either $\Delta_g(s)$ or $\Delta^{\text{re}}_g(s)$ after 7 iteration steps.

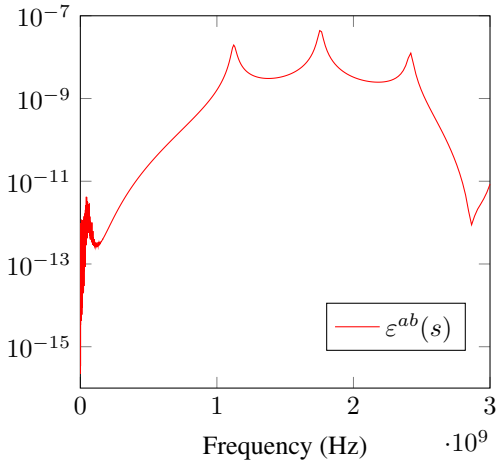

FIGURE 3. RLC tree, the true absolute error over Ξ^3_{ver}.

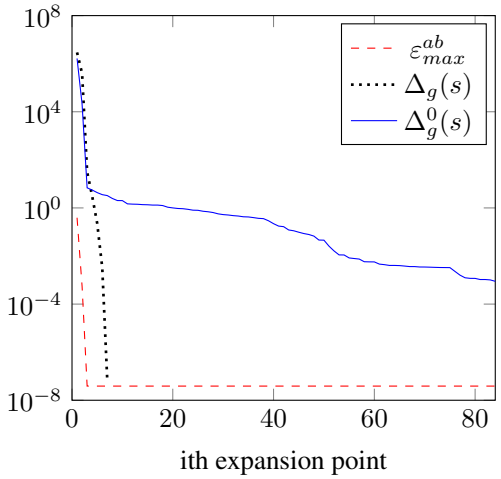

FIGURE 4. RLC tree, the behavior of $\Delta^0_g(s)$ with $V^{du} = V$.

To test the rigorousness of the error bound $\Delta_g(s)$, we plot in Figure 3 the true absolute errors of the final reduced-order model at 2700 exponentially distributed samples in $f \in [0, 3 \times 10^9]$:

$$\Xi^3_{\text{ver}} : \left\{ f_i = 3 \times 10^{(i/300)}, s_i = 2\pi\sqrt{-1} f_i, i = 1, \ldots, 2700 \right\}.$$

The errors are all below the error bound $\Delta_g(\hat{s}) = 6.64 \times 10^{-8}$ in Table 6, the error bound for the final reduced-order model derived at the last iteration step.

It is analyzed at the end of Section 4 that for Galerkin projection, the error bound $\Delta_g(s)$ using V^{du} computed from (7.6) should perform better than the error bound, say $\Delta^0_g(s)$, using $V^{du} = V$. Here we show the behavior of $\Delta^0_g(s)$ in Figure 4. With the same inputs for Algorithm 1, we compare $\Delta^0_g(s)$ in Figure 4 with $\Delta_g(s)$ in Table 6. It is obvious that $\Delta^0_g(s)$ decreases much slower than $\Delta_g(s)$. Using $\Delta_g(s)$, the algorithm constructs the final reduced-order model within 7 iteration steps; while using $\Delta^0_g(s)$, it takes 84 iterations. It is observed that the

residual of the dual system $||r^{du}||_2$ decreases at least as fast as $||r^{pr}||_2$ if $V^{du} \neq V$. However, $||r^{du}||_2$ stagnates at around O(1) for the case $V^{du} = V$, while $||r^{pr}||_2$ keeps decreasing.

8.3. Results for $\Delta_g(\mu)$ and $\tilde{\Delta}_g(\mu)$

In this subsection, we show the behavior of the error bounds $\Delta_g(\mu)$ and $\tilde{\Delta}_g(\mu)$ in Theorem 4.1 by using the parameterized system for a MEMS model, Butterfly Gyroscope [9], as an example. It is of the following form

$$\begin{aligned} M(d)\ddot{x} + D(\theta,\alpha,\beta,d)\dot{x} + T(d)x &= Bu(t), \\ y &= Cx. \end{aligned}$$

Here, $M(d) = (M_1 + dM_2)$, $T(d) = (T_1 + \frac{1}{d}T_2 + dT_3)$, $D(\theta,\alpha,\beta,d) = \theta(D_1 + dD_2) + \alpha M(d) + \beta T(d) \in R^{n\times n}$, $n = 17,913$. The parameters are d, θ, α, β.

After Laplace transform action, the system in frequency domain is

$$\begin{aligned} s^2M(d)x + sD(\theta,\alpha,\beta,d)x + T(d)x &= Bu_{\mathcal{L}}(s), \\ y &= Cx. \end{aligned}$$

The above system can be rewritten into the affine form,

$$\begin{aligned} G(\mu)x &= Bu_{\mathcal{L}}(\mu), \\ y &= Cx, \end{aligned}$$

where $G(\mu) = T_1 + \mu_1 M_1 + \mu_2 M_2 + \mu_3 D_1 + \mu_4 D_2 + \mu_5 M_1 + \mu_6 M_2 + \mu_7 T_1 + \mu_8 T_2 + \mu_9 T_3 + \mu_{10} T_2 + \mu_{11} T_3$. Here $\mu = (\mu_1, \ldots, \mu_{11})^T$ includes the newly generated parameters, $\mu_1 = s^2$, $\mu_2 = s^2 d$, $\mu_3 = s\theta$, $\mu_4 = s\theta d$, $\mu_5 = s\alpha$, $\mu_6 = s\alpha d$, $\mu_7 = s\beta$, $\mu_8 = s\beta/d$, $\mu_9 = s\beta d$, $\mu_{10} = 1/d$, $\mu_{11} = d$.

The transfer function of this system is of very small magnitude, which is in the interval $[10^{-7}, 10^{-4}]$ [21]. Therefore, the tolerance ε_{tol} for the absolute error of the reduced-order model is assigned a small value $\varepsilon_{\text{tol}} = 10^{-7}$. The tolerance ε_{tol} for the relative error is taken as $\varepsilon_{\text{tol}} = 10^{-2}$.

For this example, the training sample space is taken as Ξ^4_{train}:

$$\left\{3 \text{ random } \theta \in [10^{-7}, 10^{-5}], 10 \text{ random } s,\ 5 \text{ random } d \in [1,2], \text{and } \alpha = 0, \beta = 0\right\}.$$

The frequency range for $s = 2\pi\jmath f$ is $f \in [0.025, 0.25]KHz$, numerically $f \in [25, 250]$. There are totally 150 samples of $\mu = (\mu_1, \ldots, \mu_{11})$. It is indicated in [46], that $\alpha = 0$ and $\beta = 0$ do not affect the accuracy of the reduced-order model, therefore they are taken as zeros in Ξ^4_{train}.

8.3.1. Behavior of $\Delta_g(\mu)$

Figure 5 shows the error bound $\Delta_g(\mu)$ and the true absolute error $\varepsilon^{ab}_{\max}$ at each iteration step of Algorithm 2. The plot on the right is the effectivity $\frac{\Delta_g(\mu)}{\varepsilon^{ab}_{\max}}$, which shows the sharpness of the error bound. It is already below 10 at the final iterations in Algorithm 2, showing the error bound is close to the true error. Here R_0, R_1, R_2 in (7.3) are used for each expansion point μ^i to generate the projection matrix V, the resulting reduced-order model is of size 804, where 33 expansion points have been selected.

To further reduce the size of the reduced-order model, one may use only R_0, R_1 for each μ^i. The case is shown in Figure 6. The computed reduced-order model is of a much smaller size $r = 210$, and 36 expansion points have been selected.

To verify the reduced-order model obtained by the above two cases,

- Case 1: $V_{\mu^i} = \text{span}\{R_0, R_1, R_2\}_{\mu^i}$,
- Case 2: $V_{\mu^i} = \text{span}\{R_0, R_1\}_{\mu^i}$,

[9]Benchmark available at http://modelreduction.org.

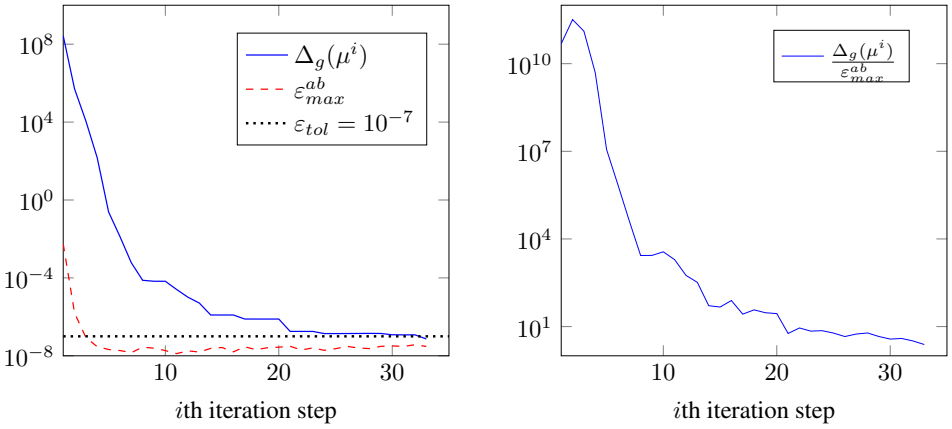

FIGURE 5. $V_{\mu^i} = \text{span}\{R_0, R_1, R_2\}_{\mu^i}$, $i = 1, \ldots, 33$. $\varepsilon_{\text{tol}} = 10^{-7}$, $r = 804$.

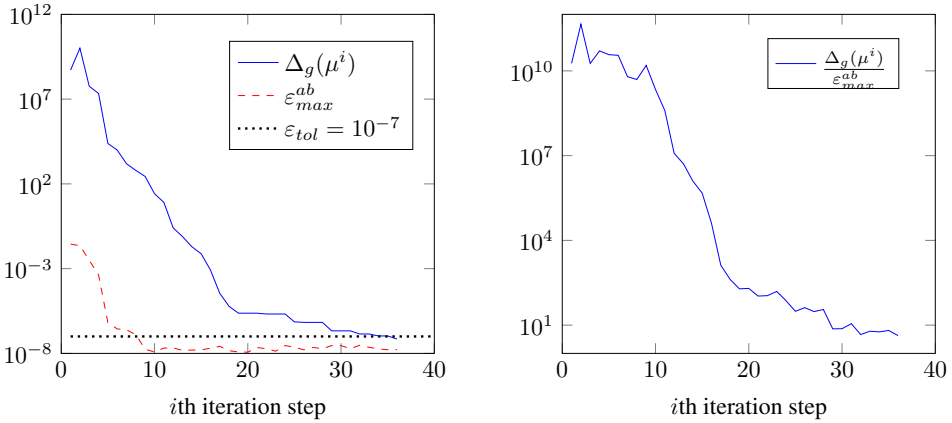

FIGURE 6. $V_{\mu^i} = \text{span}\{R_0, R_1\}_{\mu^i}$, $i = 1, \ldots, 36$, $\varepsilon_{\text{tol}} = 10^{-7}$, $r = 210$.

a much denser sample space is taken as

$$\Xi^4_{\text{ver}} : \{5 \text{ random } \theta, 50 \text{ random } s, \ 10 \text{ random } d, \text{and } \alpha = 0, \beta = 0\}.$$

There are totally 2500 samples of $\mu = (\mu_1, \ldots, \mu_{11})$. The data of the two reduced-order models are listed in Table 8. In the table, $\Delta_g(\mu^{\text{final}})$ is the value of the error bound $\Delta_g(\mu)$ at the expansion point μ^{final} selected by Algorithm 2 at the final iteration step, which is the error bound for the final reduced-order model. The true error of the reduced-order model is very close to but below $\Delta(\mu^{\text{final}})$ in each case, indicating that the error bound is both rigorous and sharp. The number of iterations indicates the total iteration steps implemented in the greedy algorithm. To evaluate the transfer function over Ξ^4_{ver}, one needs 1295 seconds if the reduced-order model of size 804 is used. Instead, only 29 seconds are needed, if the reduced-order model in the second case is used.

The relative error bound $\Delta^{\text{re}}_g(\mu)$ behaves as well as the absolute error bound. The corresponding results in Figure 7 are computed using R_0, R_1 for each expansion point. The reduced-order model is of order $r = 216$, and

TABLE 8. Verification of the final ROMs over Ξ^4_{ver}.

Cases	$\Delta_g(\mu^{\text{final}})$	$\varepsilon^{ab}_{\max}$	iterations	ROM size	time
Case 1	7.4×10^{-8}	1.77×10^{-9}	33	804	1295 s
Case 2	7.1×10^{-8}	1.4×10^{-9}	36	210	29 s

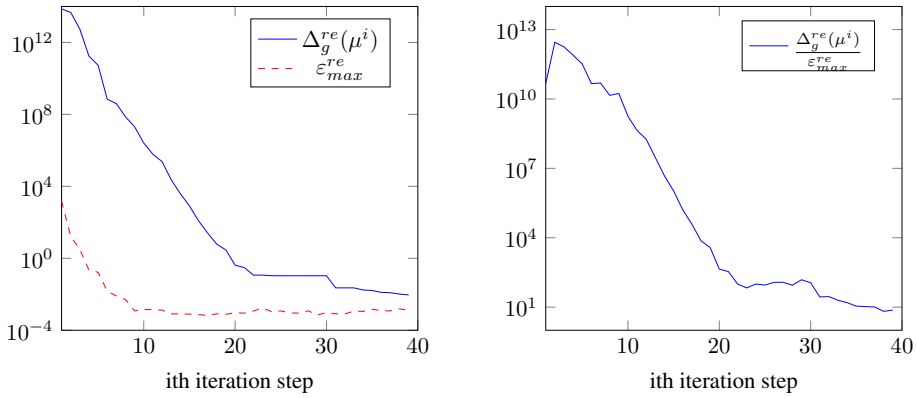

FIGURE 7. $V_{\mu^i} = \text{span}\{R_0, R_1\}_{\mu^i}$, $i = 1, \ldots, 39$, $\varepsilon_{\text{tol}} = 10^{-2}$, $r = 216$.

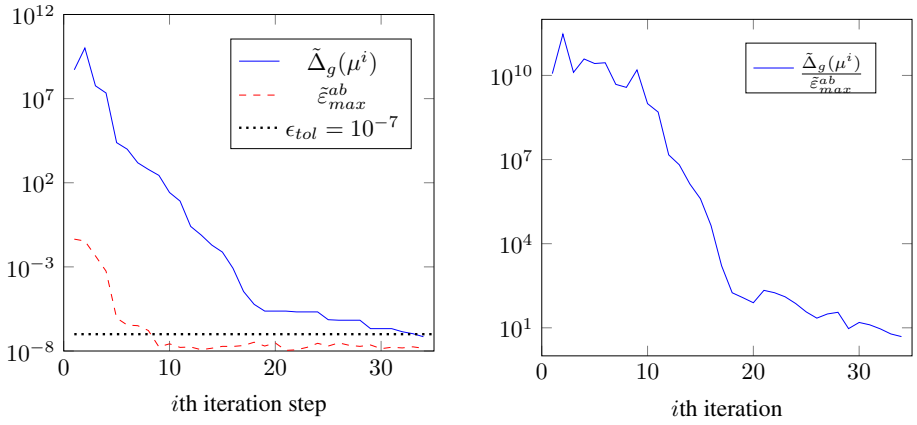

FIGURE 8. $V_{\mu^i} = \text{span}\{R_0, R_1\}_{\mu^i}$, $i = 1, \ldots, 34$, $\varepsilon_{\text{tol}} = 10^{-7}$, $r = 429$.

39 expansion points have been selected after 39 iterations. The figure again shows the robustness of the error bound.

8.3.2. Behavior of $\tilde{\Delta}_g(\mu)$

In Section 6, we propose a reformulated reduced-order model, whose transfer function is exactly $\tilde{y}(\mu)$, so that the error bound for the transfer function of the reformulated reduced-order model is $\tilde{\Delta}_g(\mu)$. Figure 8 shows the decay of $\tilde{\Delta}_g(\mu)$ with the iterations in the greedy algorithm, Algorithm 2. When compared to the error bound $\Delta_g(\mu)$ for the reduced-order model in (6.4), the error bound $\tilde{\Delta}_g(\mu)$ for the reformulated reduced-order model is sharper. When $\tilde{\Delta}_g(\mu)$ is used in the greedy algorithm, there are 34 iterations used, instead of 36 iterations for $\Delta_g(\mu)$, shown in Figure 6. However, the difference is not that big. The big difference is the size of the

TABLE 9. CDplayer, $\varepsilon_{\text{tol}} = 10^{-3}$, $q = 5$, $r = 60$.

iteration	$\hat{s}/(2\pi\jmath)$	$\varepsilon^{\text{re}}_{\max}$	$\Delta^{\text{re}}_g(\hat{s})$
1	0	61.02	8.3×10^3
2	3.61	28.43	2.10×10^3
3	48.8	8.88	3.86×10^3
4	11.8	0.74	513.7
5	94.4	0.73	199.6
6	615	0.0019	0.27
7	482	9×10^{-4}	0.02
8	1000	4.4×10^{-5}	1.27×10^{-4}

reduced-order models. The reformulated reduced-order model is of size $r = 429$, while the reduced-order model obtained using $\Delta_g(\mu)$ is of size $r = 216$.

8.4. Sharpness of the error bounds

It can be seen that for the examples studied, the error bounds $\Delta(s)$ and $\Delta_g(s)$ are not sharp at most iterations of the greedy algorithm. One key reason might be the values $\alpha(s)$, $\gamma(s)$ in the denominator of $\Delta(s)$, and the value $\beta(s)$ on the denominator of $\Delta_g(s)$ are too small. In Section 8.1, $\alpha(s)$ is around $O(10^{-9})$ and $\gamma(s)$ is at $O(10^{-13})$ for the second example, the optical filter. For the first example, the spiral inductor, $\gamma(s)$ is at $O(10^{-13})$, though $\alpha(s)$ is around $O(10^{-3})$.

In Section 8.2, $\beta(s)$ in $\Delta_g(s)$ is around 1×10^{-4}. If we use another example to check $\Delta_g(s)$, it behaves much better. The example is a model of a CD-player, of size $n = 120$. We use a sample space of 200 samples:

$$\Xi_{\text{train}} = \{s_i = 2\pi\sqrt{-1}f_i, f_i \in [0, 1000], i = 1, \ldots, 200\},$$

in Algorithm 1. Here f_i are logarithmically equally spaced points generated using the command `logspace(0,3,200)` in MATLAB. It is observed that the values of $\beta(s)$ at all the samples of s are between 0.2 and 700. The decay of the error bound $\Delta_g(s)$ with the iterations in the greedy algorithm is listed in Table 9. Compared with the results of $\Delta_g(s)$ in Table 7, the error bound is much sharper.

Notice that in the beginning, either the error bound $\Delta_g(\mu)$ or $\tilde{\Delta}_g(\mu)$ for the parametrized LTI systems is actually not sharp at all, this is also because the smallest singular value $\beta(\mu)$ of the matrix $G(\mu)$, which appears in the denominator of the error bound, is very small, around $O(10^{-8})$. With the iterations in the greedy algorithm going on, the two residuals in the numerator decrease very fast, so that the error bound quickly becomes much sharper.

It should be pointed out that the greedy algorithm is used to construct the reduced-order model, hence the final reduced-oder model is only available at the last iteration step of the algorithm. The reduced-order models at the intermediate iterations are less important than the reduced-order model at the final iteration step. What does matter is that the error of the finally derived reduced-order model is not only below the acceptable tolerance ε_{tol}, but also closely estimated by the error bound. Therefore, the sharpness of the error bound at the last iteration step is of most importance.

9. CONCLUSIONS

In this work, we proposed some *a posteriori* error bounds for reduced-order modeling of linear (parametrized) systems. The error bound $\Delta(s)$ for non-parametrized first-order LTI systems with symmetric negative definite A and symmetric positive definite E can be cheaply computed, so that the reduced-order model can be constructed efficiently. Computation of the error bound $\Delta_g(\mu)$ requires solving an eigenvalue problem for each sample in the training sample space. More efficient and robust methods for computing or estimating $\Delta_g(\mu)$ will be studied

in the future. The error bounds are rigorous. The sharpness of the error bounds depends, nevertheless, on the properties of the system matrices. It is demonstrated that with the guidance of any of the proposed error bounds, the reduced-order models computed with moment-matching MOR methods can be generated automatically and reliably. It is possible that the error bound $\Delta(\mu)$ or $\Delta_g(\mu)$ may realize automatic implementation of other MOR methods which are based on approximation of the transfer function.

References

[1] R. Achar and M.S. Nakhla, Simulation of high-speed interconnects. *Proc. IEEE* **89** (2001) 693–728.

[2] A.C. Antoulas, P. Benner and L. Feng, Model reduction by iterative error-system approximation (2014).

[3] D. Amsallem and C. Farhat, An online method for interpolating linear parametric reduced-order models. *SIAM J. Sci. Comput.* **33** (2011) 2169–2198.

[4] Z. Bai, R.D. Slone, W.T. Smith and Q. Ye, Error bound for reduced system model by Padé approximation via the Lanczos process. *Comput.-Aid. Design Integr. Circuits Syst.* **18** (1999) 133–141.

[5] U. Baur and P. Benner, Model reduction for parametric systems using balanced truncation and interpolation. *at–Automatisierungstechnik* **57** (2009) 411–419.

[6] U. Baur, C. Beattie, P. Benner and S. Gugercin, Interpolatory projection methods for parameterized model reduction. *SIAM J. Sci. Comput.* **33** (2011) 2489–2518.

[7] U. Baur, P. Benner and L. Feng, Model order reduction for linear and nonlinear systems: a system-theoretic perspective. *Archives Comput. Methods Eng.* **21** (2014) 331–358.

[8] T. Bechtold, E.B. Rudnyi and J.G. Korvink, Error indicators for fully automatic extraction of heat-transfer macromodels for MEMS. *Micromech. Microeng.* **15** (2005) 430–440.

[9] P. Benner, System-theoretic methods for model reduction of large-scale systems: simulation, control, and inverse Problems. In vol. 35 of *Proc. of MATHMOD 2009, 6th Vienna International Conference on Mathematical Modelling*, ARGESIM Report (2009) 126–145.

[10] P. Benner, S. Gugercin and K. Willcox, A survey of projection-based model reduction methods for parametric dynamical systems. *SIAM Rev.* **57** (2015) 483–531.

[11] P. Benner and L. Feng, A robust algorithm for parametric model order reduction based on implicit moment matching. In: Reduced Order Methods for modeling and computational reduction, edited by A. Quateroni, G. Rozza. Vol. 9 of Springer MS&A series (2014) 159–185.

[12] A. Bodendiek and M. Bollhöfer, Adaptive-order rational Arnoldi-type methods in computational electromagnetism. *BIT Numer. Math.* **54** (2014) 357–380.

[13] T. Bonin, H. Fassbender, A. Soppa and M. Zaeh, A fully adaptive rational global Arnoldi method for the model-order reduction of second-order MIMO systems with proportional damping. *Math. Comput. Simul.* **122** (2016) 1–19.

[14] S. Boyaval, *Mathematical modelling and numerical simulation in materials science*. Ph.D. thesis, Université Paris-Est (2009).

[15] Y. Choi, D. Amsallem and C. Farhat, Gradient-Based Constrained Optimization Using a Database of Linear Reduced-Order Models. Preprint arXiv:1506.07849 (2015).

[16] L. Daniel, O.C. Siong, L.S. Chay, K.H. Lee and J. White, A multiparameter moment-matching model-reduction approach for generating geometrically parameterized interconnect performance models. *IEEE Trans. Comput.-Aid. Design Integr. Circuits Syst.* **23** (2004) 678–693.

[17] L. Feng, D. Koziol, E. Rudnyi and J.G. Korvink, Model order reduction for scanning electrochemical microscope: The treatment of nonzero initial condition. In vol. 3 of *Proc. of Sensors* **3** (2004) 1236–1239.

[18] L. Feng, E.B. Rudnyi and J.G. Korvink, Preserving the film coefficient as a parameter in the compact thermal model for fast electrothermal simulation. *IEEE Trans. Computer-Aided Design of Integrated Circuits and Systems* **24** (2005) 1838–1847.

[19] L. Feng and P. Benner, A robust algorithm for parametric model order reduction. *Proc. Appl. Math. Mech.* **7** (2017) 1021501–1021502.

[20] L. Feng, J.G. Korvink and P. Benner, A fully adaptive scheme for model order reduction based on moment-matching. *IEEE Trans. Components, Packaging Manuf. Technol.* **5** (2015) 1872–1884.

[21] L. Feng, P. Benner and J.G. Korvink, Subspace recycling accelerates the parametric macro-modeling of MEMS. *Inter. J. Numer. Methods Eng.* **94** (2013) 84–110.

[22] R.W. Freund, Model reduction methods based on Krylov subspaces. *Acta Numer.* **12** (2003) 267–319.

[23] E.J. Grimme, *Krylov projection methods for model reduction*. Ph.D. thesis, Univ. Illinois, Urbana Champaign (1997).

[24] M. Grepl, *Reduced-basis approximation and a posteriori error estimation for parabolic partial differential equations*. Ph.D. thesis, Massachusetts Institute of Technology (2005).

[25] M.A. Grepl and A.T. Patera, *A posteriori* error bounds for reduced-basis approximations of parametrized parabolic partial differential equations. *ESAIM: M2AN* **39** (2005) 157–181.

[26] S. Gugercin, A. C. Antoulas and C. A. Beattie, $\mathcal{H}_2$ model reduction for large-scale linear dynamical systems. *SIAM J. Matrix Anal. Appl.* **30** (2008) 609–638.

[27] J. S. Hesthaven, B. Stamm and S. Zhang, Efficient greedy algorithms for high-dimensional parameter spaces with applications to empirical interpolation and reduced basis methods. *ESAIM: M2AN* **48** (2014) 259–283.

[28] J.S. Hesthaven, G. Rozza and B. Stamm, Certified Reduced Basis Methods for Parametrized Partial Differential Equations. *SpringerBriefs in Mathematics*. Springer (2016).

[29] U. Hetmaniuk, R. Tezaur and C. Farhat. An adaptive scheme for a class of interpolatory model reduction methods for frequency response problems. *Inter. J. Numer. Methods Eng.* **93** (2013) 1109–1124.

[30] B. Haasdonk and M. Ohlberger. Efficient reduced models for parametrized dynamical systems by offline/online decomposition. *In Proc. of MATHMOD 2009, 6th Vienna International Conference on Mathematical Modelling* (2009).

[31] D.B.P. Huynh, G. Rozza, S. Sen and A.T. Patera, A successive constraint linear optimization method for lower bounds of parametric coercivity and inf-sup stability constants. *Comput. Rendus Math.* **345** (2007) 473–478.

[32] N. Jung, A.T. Patera, B. Haasdonk and B. Lohmann, Model order reduction and error estimation with an application to the parameter-dependent eddy current equation. *Math. Comput. Model. Dynamical Syst.* **17** (2011) 561–582.

[33] H.-J. Lee, Ch.-Ch. Chu and W.-Sh. Feng, An adaptive-order rational Arnoldi method for model-order reductions of linear time-invariant systems. *Lin. Algebra Appl.* **415** (2006) 235–261.

[34] T.H. Lee. The design of CMOS radio-frequency integrated circuits, 2nd ed. Cambridge UK: Cambridge University Press (2004).

[35] S. Lefteriu, A.C. Antoulas and A.C. Ionita, Parametric model reduction in the Loewner framwork. *In Proc. of 18th IFAC World Congress* (2011) 12752–12756.

[36] B.C. Moore, Principal component analysis in linear systems: controllability, observability, and model reduction. *IEEE Trans. Automatic Control* **AC-26** (1981) 17–32.

[37] H. Panzer, J. Mohring, R. Eid and B. Lohmann, Parametric model order reduction by matrix interpolation. *at-Automatisierungstechnik* **58** (2010) 475–484.

[38] A. Odabasioglu, M. Celik and L.T. Pileggi, PRIMA: passive reduced-order interconnect macromodeling algorithm. *IEEE Trans. Comput.-Aid. Design Integr. Circuits Syst.* **17** (1998) 645–654.

[39] D.V. Rovas, *Reduced-basis output bound methods for parametrized partial differential equations*. Ph.D. thesis, Massachusetts Institute of Technology (2003).

[40] G. Rozza, D.B.P. Huynh and A.T. Patera, Reduced basis approximation and a posteriori error estimation for affinely parametrized elliptic coercive partial differential equations. *Archives Comput. Methods Eng.* **15** (2008) 229–275.

[41] E.B. Rudnyi and J.G. Korvink, Model order reduction for large scale engineering models developed in ANSYS. In vol. 3732 of *Lect. Notes Comput. Sci.* Springer Verlag (2006) 349–356.

[42] S. Sen, *Reduced basis approximation and a posteriori error estimation for non-coercive elliptic problems*. Ph.D. thesis, Massachusetts Institute of Technology (2007).

[43] T. Wolf, H. Panzer and B. Lohmann, Gramian-based error bound in model reduction by Krylov subspace methods. *In Proc. of IFAC World Congress* **44** (2011) 3587–3592.

[44] P.K. Gunupudi, R. Khazaka, M.S. Nakhla, T. Smy and D. Celo, Passive parameterized time-domain macromodels for high-speed transmission-line networks. *IEEE Trans. Microwave Theory Tech.* **51** (2003) 2347–2354.

[45] Y.-T. Li, Z. Bai, Y.-F. Su and X. Zeng, Model order reduction of parameterized interconnect networks via a two-directional Arnoldi process. *Comput.-Aid. Design Integr. Circuits Syst.* **27** (2008) 1571–1582.

[46] B. Salimbahrami, R. Eid and B. Lohmann, Model reduction by second order Krylov subspaces: extensions, stability and proportional damping. *In Proc. of IEEE Conference on Computer Aided Control Systems Design* (2006) 2997–3002.

[47] A. Paul−Dubois−Taine and D. Amsallem. An adaptive and efficient greedy procedure for the optimal training of parametric reduced-order models. *Inter. J. Numer. Methods Eng.* **102** (2014) 1262–1292.

[48] K. Urban and A.T. Patera, An improved error bound for reduced basis approximation of linear parabolic problems. *Math. Comput.* **83** (2014) 1599–1615.

[49] M. Yano, A space-time Petrov-Galerkin certified reduced basis method: Application to the Boussinesq equations. *SIAM J. Sci. Comput.* **36** (2014) A232–A266.

[50] M. Yano, A.T. Patera and K. Urban, A space-time hp-interpolation-based certified reduced basis method for Burgers' equation. *Math. Models Methods Appl. Sci.* **24** (2014) 1903–1935.

[51] Y. Zhang, L. Feng, S. Li and P. Benner, An efficient output error estimation for model order reduction of parametrized evolution equations. *SIAM J. Sci. Comput.* **37** (2015) B910–B936.